OPEN ACCESS
IOP Publishing
Journal of Physics A: Mathematical and Theoretical
J. Phys. A: Math. Theor. **58** (2025) 205302 (27pp)
https://doi.org/10.1088/1751-8121/add4d3

On the non-hermitian Kitaev chain

Eddy Ardonne* **and Viktor Kurasov**

Department of Physics, Stockholm University, AlbaNova University Center, 106 91 Stockholm, Sweden

E-mail: ardonne@fysik.su.se

Received 28 November 2024; revised 9 April 2025
Accepted for publication 6 May 2025
Published 14 May 2025

Abstract

We study the non-hermitian Kitaev chain model, for arbitrary complex parameters. In particular, we give a concise characterization of the curves of eigenvalues in the complex plane in the infinite size limit, using a novel method which can be applied to other non-hermitian systems. Using this solution, we characterize under which conditions the skin effect is absent, and for which eigenstates this is the case. We also fully determine the region in parameter space for which the model has a zero mode.

Keywords: Kitaev chain, non-hermitian systems, zero modes, skin effect

1. Introduction

The study of non-hermitian systems, in various contexts, has been extremely intense during the last years. These studies cover the properties of non-hermitian systems in general (focussing on the differences and similarities with hermitian systems), studies of particular non-hermitian models, as well as utilizing non-hermitian systems for actual applications, using various different types of physical systems [1–52]. One aspect that is of particular relevance for the current paper is the presence of the skin-effect, which is closely related to the breakdown of the famed bulk boundary correspondence of hermitian topological systems [53–65].

In this paper, we focus solely on Kitaev chain [66] famous for its Majorana zero modes in its topological phase (see [67] for a review). We consider the non-hermitian version of this model, which has, in various incarnations, been studied before [68–86]. A main result is that we concisely characterize the location of the eigenvalues in the complex plane in the limit for an open chain in the infinite system size. Using our novel method, we can explain why the

* Author to whom any correspondence should be addressed.

curves the eigenvalues lie on exhibit branch points. Using our solution, we can address several other interesting questions.

It is clearly natural to ask for which general choice of parameters does the non-hermitian Kitaev chain have a zero-mode. Interestingly, the full answer to this question is arguably a bit more complicated than one might expect.

The eigenvalues of generic non-hermitian systems are known to be very sensitive to the boundary conditions [14, 16]. This is due to the skin effect. Eigenstates exhibiting the skin effect are localized at the boundary of the system, with an amplitude that decays exponentially in the bulk of the system. Because of this exponential localization of the eigenstates near the boundary, it is clear that the system will be sensitive to small changes in the boundary conditions. In addition, the usual algorithms to obtain the eigenvalues numerically becomes unstable for large system sizes. For one-dimensional systems, one can use knowledge of the periodic system in order to predict whether or not the open system exhibit skin-effect or not. In particular, one considers the eigenvalues of the periodic system, and determines if this winds around an arbitrary point [11, 13, 34]. If such a winding exists, the system exhibits a skin effect. It is, however, not *a priori* clear for which choices of parameters in the model this occurs, and if it occurs, to which eigenvalues it pertains. Because of this, it is interesting to find an exact solution of the non-hermitian model one studies. By this we mean a concise characterization of the eigenvalues, that can be easily solved numerically, without stability issues.

In the current paper, we use our novel method to obtain the eigenvalues in the thermodynamic limit in order to provide explicit answers to the questions we posed above for the non-hermitian Kitaev chain. We introduce the non-hermitian Kitaev chain, in order to set the notation, and start with the general analysis to solve the model in section 2. We continue in section 3 by providing the solution of the non-hermitian Kitaev chain, for *chains of finite length*, under the restriction that the left and right hopping parameters t_1 and t_2 are equal. In section 4 we give a complete characterization of the parameters, for which the (non-hermitian) model has a zero-mode. Here, we directly work in the infinite system size limit. In section 5, we provide a concise characterization of the eigenvalues of the model, again for fully generic parameters, in the infinite system size limit. Using this characterization, one can easily obtain the curves in the complex plain corresponding to the eigenvalues of the model. In section 6, we analyze the solution to determine under which conditions the model exhibits skin effect, and if this is the case, to which eigenvalues this pertains. In section 7 we summarize our results by means of an example, followed by a short discussion in section 8.

2. The non-hermitian Kitaev chain

In this section we state the model we are interested in, namely the Kitaev chain [66] with nearest neighbor hopping and pairing, for arbitrary, complex parameters and start with the analysis to find the eigenvalues. We are mainly interested in open chains, with 'free' boundary conditions. In this paper, we do not study the transition from the open to the periodic system. In terms of fermion creation and annihilation operators, $c_j^\dagger$, c_j, the model for L sites reads

$$H = \sum_{j=1}^{L} \frac{m}{2}\left(c_j^\dagger c_j - c_j c_j^\dagger\right) + \sum_{j=1}^{L-1}\left(t_1 c_j^\dagger c_{j+1} + t_2 c_{j+1}^\dagger c_j + d_1 c_j^\dagger c_{j+1}^\dagger + d_2 c_{j+1} c_j\right) . \tag{1}$$

If the model were hermitian, m would take the role of the chemical potential, t_1 and t_2 would be the hopping parameters, while d_1 and d_2 would correspond to the superconducting order parameter.

To analyze the model, we write the hamiltonian in Bogoliubov-de Gennes form, that is, we write

$$H = \frac{1}{2}\Psi^\dagger \cdot \mathcal{H}_{\mathrm{BdG}} \cdot \Psi \ , \tag{2}$$

where $\Psi^\dagger = (c_1^\dagger, c_1, c_2^\dagger, c_2, \ldots)$. For the model equation (1), we find that $\mathcal{H}_{\mathrm{BdG}}$ is the following $2L \times 2L$ matrix

$$\mathcal{H}_{\mathrm{BdG}} = \begin{pmatrix}
m & 0 & t_1 & d_1 & 0 & 0 & \cdots & \cdots & 0 & 0 \\
0 & -m & -d_2 & -t_2 & 0 & 0 & \cdots & \cdots & 0 & 0 \\
t_2 & -d_1 & m & 0 & t_1 & d_1 & & & \vdots & \vdots \\
d_2 & -t_1 & 0 & -m & -d_2 & -t_2 & & & \vdots & \vdots \\
0 & 0 & t_2 & -d_1 & m & 0 & \ddots & & 0 & 0 \\
0 & 0 & d_2 & -t_1 & 0 & -m & & \ddots & 0 & 0 \\
\vdots & \vdots & & & \ddots & & \ddots & & t_1 & d_1 \\
\vdots & \vdots & & & & \ddots & & \ddots & -d_2 & -t_2 \\
0 & 0 & \cdots & \cdots & 0 & 0 & t_2 & -d_1 & m & 0 \\
0 & 0 & \cdots & \cdots & 0 & 0 & d_2 & -t_1 & 0 & -m
\end{pmatrix} . \tag{3}$$

We thus need to find the eigenvalues λ of this matrix with arbitrary parameters m, t_1, t_2, d_1, d_2.

To this end, we write $\mathcal{H}_{\mathrm{BdG}}\psi = \lambda\psi$ and we denote the components of ψ by ψ_n. The eigenvalue equations give rise to $2L-4$ bulk equations (with $n = 3, \ldots 2L-2$),

$$\begin{cases} t_2\psi_{n-2} - d_1\psi_{n-1} + (m-\lambda)\psi_n + t_1\psi_{n+2} + d_1\psi_{n+3} = 0 & \text{for } n \text{ odd} \\ d_2\psi_{n-3} - t_1\psi_{n-2} + (-m-\lambda)\psi_n - d_2\psi_{n+1} - t_2\psi_{n+2} = 0 & \text{for } n \text{ even} \ . \end{cases} \tag{4}$$

In addition, there are four boundary equations which read, after using the bulk equations (which we will always solve for arbitrary integer n)

$$\begin{aligned} -t_2\psi_{-1} + d_1\psi_0 &= 0 & \qquad -t_1\psi_{2L+1} - d_1\psi_{2L+2} &= 0 \\ -d_2\psi_{-1} + t_1\psi_0 &= 0 & \qquad +d_2\psi_{2L+1} + t_2\psi_{2L+2} &= 0 \ . \end{aligned} \tag{5}$$

To obtain the eigenvalues λ, we use the following concrete ansats for the components of the (right) eigenvectors,

$$\psi^T = \phi^T(x,a) = \left(x, ax, x^2, ax^2, \ldots, x^L, ax^L\right) \ . \tag{6}$$

This ansatz is inspired by the ansatz used in the hermitian case, where a in general is a phase (due to the superconducting nature of the model). Because we deal with the non-hermitian case, a will have arbitrary modulus. The structure of the powers of x is the standard ansatz used in solving the type of recurrence relations for the bulk of systems with periodicity. In the physics literature, this dates back at least to the seminal paper of Lieb *et al* [87]. Using this ansatz, the 'bulk' equations take the following form,

$$t_2 - ad_1 + (m-\lambda)x + (t_1 + ad_1)x^2 = 0 \qquad d_2 - at_1 + (-m-\lambda)ax + (-d_2 - at_2)x^2 = 0 \ . \tag{7}$$

By eliminating a from these equations, one obtains a fourth order algebraic equation in x,

$$\begin{aligned}(d_1d_2-t_1t_2)\,x^4-(\lambda\,(t_1-t_2)+m\,(t_1+t_2))\,x^3+\left(\lambda^2-m^2-2d_1d_2-t_1^2-t_2^2\right)x^2\\+(\lambda\,(t_1-t_2)-m\,(t_1+t_2))\,x+(d_1d_2-t_1t_2)=0\,.\end{aligned}\tag{8}$$

Thus (because the value for a is uniquely determined by a given solution for x), we obtain four solutions of the bulk equations, denoted by (x_i,a_i). The general form of the eigenvector then is $\psi=\sum_{i=1}^{4}c_i\,\phi(x_i,a_i)$. The coefficients c_i can be obtained from the boundary equations, which now take the form

$$\begin{aligned}(-t_2+a_1d_1)\,c_1+(-t_2+a_2d_1)\,c_2+(-t_2+a_3d_1)\,c_3+(-t_2+a_4d_1)\,c_4=0\\(-d_2+a_1t_1)\,c_1+(-d_2+a_2t_1)\,c_2+(-d_2+a_3t_1)\,c_3+(-d_2+a_4t_1)\,c_4=0\\-(t_1+a_1d_1)\,x_1^{L+1}c_1-(t_1+a_2d_1)\,x_2^{L+1}c_2-(t_1+a_3d_1)\,x_3^{L+1}c_3-(t_1+a_4d_1)\,x_4^{L+1}c_4=0\\(d_2+a_1t_2)\,x_1^{L+1}c_1+(d_2+a_2t_2)\,x_2^{L+1}c_2+(d_2+a_3t_2)\,x_3^{L+1}c_3+(d_2+a_4t_2)\,x_4^{L+1}c_4=0\,.\end{aligned}\tag{9}$$

In practise, one typically does not obtain the explicit values of the c_i, but instead uses these equations to determine the eigenvalues. The pairs (x_i,a_i) implicitly depend on λ and the parameters in the model. The condition that the boundary equations have a non-trivial solution for the c_i then turns into an equation for the possible eigenvalues λ. In particular, we write the equations as $Mc=0$, where $c^T=(c_1,c_2,c_3,c_4)$ and

$$M=\begin{pmatrix}-t_2+a_1d_1 & -t_2+a_2d_1 & -t_2+a_3d_1 & -t_2+a_4d_1\\ -d_2+a_1t_1 & -d_2+a_2t_1 & -d_2+a_3t_1 & -d_2+a_4t_1\\ -(t_1+a_1d_1)\,x_1^{L+1} & -(t_1+a_2d_1)\,x_2^{L+1} & -(t_1+a_3d_1)\,x_3^{L+1} & -(t_1+a_4d_1)\,x_4^{L+1}\\ (d_2+a_1t_2)\,x_1^{L+1} & (d_2+a_2t_2)\,x_2^{L+1} & (d_2+a_3t_2)\,x_3^{L+1} & (d_2+a_4t_2)\,x_4^{L+1}\end{pmatrix}.\tag{10}$$

The condition to have a non-trivial solution for the c_i is $\det(M)=0$, which determines λ via the parameters (x_i,a_i). In the sections below, we perform the analysis to characterize λ for various different cases.

Before doing so, we mention, for later use, that the eigenvalues λ of the periodic version of the model take a simple form in terms of the momentum k, namely

$$\lambda_{\pm}(k)=\mathrm{i}\,(t_1-t_2)\sin(k)\pm\sqrt{4d_1d_2\sin(k)^2+(m+(t_1+t_2)\cos(k))^2}\,.\tag{11}$$

These eigenvalues corresponding to the model with periodic boundary conditions are obtained by first performing a (discrete) Fourier transform. This results in the following 2×2 matrix

$$\begin{pmatrix}m+t_1\mathrm{e}^{\mathrm{i}k}+t_2\mathrm{e}^{-\mathrm{i}k} & d_1\left(\mathrm{e}^{\mathrm{i}k}+\mathrm{e}^{-\mathrm{i}k}\right)\\ -d_2\left(\mathrm{e}^{\mathrm{i}k}+\mathrm{e}^{-\mathrm{i}k}\right) & -m-t_1\mathrm{e}^{-\mathrm{i}k}-t_2\mathrm{e}^{\mathrm{i}k}\end{pmatrix}.\tag{12}$$

The eigenvalues of this matrix are indeed given by equation (11).

3. Solution for finite L, with $t_2 = t_1$ or $d_1 d_2 = 0$

In this section, we start by presenting the full solution of the model, for an open chain of size L, but with the restriction that $t_2 = t_1$. In this section, we use the notation $t = t_1 = t_2$, to remind the reader of this restriction. We use the method of Lieb *et al* [87], which was used to study the hermitian Kitaev chain with longer range hopping in [88]. We use the approach taken in the latter paper, or rather, repeat the calculation. We only need to note that the restriction used in that paper, namely that the chemical potential and the hopping parameter are real, can in fact be dropped, without invalidating the solution. Thus, we allow complex parameters $m, t = t_1 = t_2, d_1, d_2$. We note these parameters *do not* include all the hermitian cases, the hermitian case with complex hopping parameters is excluded. However, the solution *does* include non-hermitian cases.

Thus, the goal of this section is to describe the eigenvalues of the matrix $\mathcal{H}_{\mathrm{BdG}}$ of equation (3), with (possibly complex) parameters $m, t = t_1 = t_2, d_1, d_2$. Here, we are very brief, and refer to [88] for the details.

We write the ansatz for the eigenvalues as $\lambda_\alpha = \pm\sqrt{4d_1 d_2 \sin^2(\alpha) + (m + 2t\cos(\alpha))^2}$, inspired by the solution for the periodic case with $t = t_1 = t_2$, equation (11). To find the values of α, we have to solve the 'bulk' equation equation (8), for the wave functions. The 'boundary' equations then give two equations that determine α. The bulk equation actually has four solutions, $\mathrm{e}^{\mathrm{i}\alpha}$, $\mathrm{e}^{-\mathrm{i}\alpha}$, $\mathrm{e}^{\mathrm{i}\beta}$, $\mathrm{e}^{-\mathrm{i}\beta}$, where the values of α and β are related by the following equation

$$2\cos(\alpha) + 2\cos(\beta) = \frac{2mt}{d_1 d_2 - t^2}\,. \tag{13}$$

Often, we introduce the notation $x = \mathrm{e}^{\mathrm{i}\alpha}$ and $y = \mathrm{e}^{\mathrm{i}\beta}$, because in this way, the equations for x and y are polynomial equations, while those for α and β are trigonometric.

The boundary equations lead to a determinant that should be zero, $\det(M) = 0$ with M given by equation (10), giving the second equation that we need to determine α and β (or x and y). To describe this equation, we introduce the following sine ratios

$$\mathrm{sr}(L, \alpha) = \frac{\sin(L\alpha)}{\sin(\alpha)} = x^{-L+1} + x^{-L+3} + \cdots + x^{L-3} + x^{L-1}\,, \tag{14}$$

and similar for β and y. Using these functions, the determinant equation takes the following form

$$\left(d_1 d_2 - t^2\right)\mathrm{sr}(L+1, \alpha)\,\mathrm{sr}(L+1, \beta) + 4d_1 d_2 \sum_{j=1}^{L} (L + 1 - j)\,\mathrm{sr}(j, \alpha)\,\mathrm{sr}(j, \beta) = 0\,. \tag{15}$$

We note that the equivalent equation in [88] takes a different (and more complicated) form, because here, we simplified the boundary equations before forming the determinant equation that finally gives the solutions.

To determine the eigenvalues λ_α, we need to solve equations (13) and (15) simultaneously. These equations are (separately) invariant under $x \leftrightarrow y$, $x \leftrightarrow 1/x$ and $y \leftrightarrow 1/y$. So, the $8L$ solutions of these equations correspond to L plus/minus eigenvalue pairs, so $2L$ eigenvalues as needed.

We note that the functions $\mathrm{sr}(L, \alpha)$ are, by definition, closely related to the Chebyshev polynomials of the second kind U_n, namely $\mathrm{sr}(L, \alpha) = U_L(\cos\alpha)$ [89]. Also, the sum over j in

equation (15) 'can be done', leading to the following result

$$\left(d_1 d_2 - t^2\right) \mathrm{sr}\left(L+1,\alpha\right) \mathrm{sr}\left(L+1,\beta\right) + \frac{d_1 d_2}{\left(\cos\alpha - \cos\beta\right)^2} \left(2 - 2\mathrm{sr}\left(L+1,\alpha\right) \mathrm{sr}\left(L+1,\beta\right) + \mathrm{sr}\left(L+2,\alpha\right) \mathrm{sr}\left(L,\beta\right) + \mathrm{sr}\left(L,\alpha\right) \mathrm{sr}\left(L+2,\beta\right)\right) = 0 \,. \tag{16}$$

Before continuing the analysis of the model for infinite system size, we briefly consider the case with either $d_1 = 0$ or $d_2 = 0$, but not necessarily both, and otherwise arbitrary parameters (so we allow $t_1 \neq t_2$ here). In this case, the model is closely related to the Hatano-Nelson model [90–92], for which an exact solution that interpolates between open and periodic boundary conditions was presented in [65]. Using the techniques of that paper, we find that for $d_2 = 0$, the eigenvalues do not depend on d_1 (and the other way around), but a subset of the eigenvectors does depend on d_1. The eigenvalues are given by

$$\lambda_{\pm,j} = \pm m + 2\sqrt{t_1}\sqrt{t_2}\cos\left(\frac{j\pi}{L+1}\right) \,, \tag{17}$$

for $j = 1, 2, \ldots, L$. We already note that for $d_1 = 0$ or $d_2 = 0$, the system does not have an isolated zero mode, and the eigenvectors show skin-effect when $|t_1| \neq |t_2|$. Finally, we note that in the case $d_1 d_2 = 0$, we can easily take the limit $L \to \infty$. That is, the eigenvalues in the infinite size limit form two line segments in the complex plane.

4. Condition for the presence of zero modes

In this section, we determine under which conditions the model has a zero mode. Just as in the hermitian Kitaev chain [66], the zero modes exhibit an exponential decay away from the boundaries, and correspond to topological edge states.

We consider arbitrary complex parameters, and work directly in the $L \to \infty$ limit. In finite systems, the energy of a zero mode decays exponentially with system size, but because we work in the limit $L \to \infty$, we put $\lambda = 0$ identically. For $\lambda = 0$, it turns out that one can obtain the solutions of the bulk equations, equation (7), explicitly

$$x_{-,-} = \frac{-m - \sqrt{4d_1 d_2 + m^2 - 4t_1 t_2}}{(t_1 + t_2) - \sqrt{4d_1 d_2 + (t_1 - t_2)^2}} \qquad a_- = \frac{-(t_1 - t_2) - \sqrt{4d_1 d_2 + (t_1 - t_2)^2}}{2d_1} \tag{18}$$

$$x_{+,-} = \frac{-m + \sqrt{4d_1 d_2 + m^2 - 4t_1 t_2}}{(t_1 + t_2) - \sqrt{4d_1 d_2 + (t_1 - t_2)^2}} \qquad a_- = \frac{-(t_1 - t_2) - \sqrt{4d_1 d_2 + (t_1 - t_2)^2}}{2d_1} \tag{19}$$

$$x_{-,+} = \frac{-m - \sqrt{4d_1 d_2 + m^2 - 4t_1 t_2}}{(t_1 + t_2) + \sqrt{4d_1 d_2 + (t_1 - t_2)^2}} \qquad a_+ = \frac{-(t_1 - t_2) + \sqrt{4d_1 d_2 + (t_1 - t_2)^2}}{2d_1} \tag{20}$$

$$x_{+,+} = \frac{-m + \sqrt{4d_1 d_2 + m^2 - 4t_1 t_2}}{(t_1 + t_2) + \sqrt{4d_1 d_2 + (t_1 - t_2)^2}} \qquad a_+ = \frac{-(t_1 - t_2) + \sqrt{4d_1 d_2 + (t_1 - t_2)^2}}{2d_1} \,, \tag{21}$$

where $x_{+,+} = 1/x_{-,-}$ and $x_{-,+} = 1/x_{+,-}$.

We can now take linear combinations of these solutions, to satisfy the boundary equations. We solve the left boundary equations exactly, and demand that $|x| < 1$, so that the right boundary equations are satisfied in the thermodynamic limit.

We find the following two solutions

$$\Psi_-^T = \phi^T(x_{-,-}, a_-) - \phi^T(x_{+,-}, a_-) \tag{22}$$

$$\Psi_+^T = \phi^T(x_{-,+}, a_+) - \phi^T(x_{+,+}, a_+)\ . \tag{23}$$

In order to satisfy the boundary equations on the right hand side, we need that either $|x_{-,-}| < 1$ and $|x_{+,-}| < 1$ such that Ψ_-^T is a zero mode or that $|x_{-,+}| < 1$ and $|x_{+,+}| < 1$ such that Ψ_+^T is a zero mode. This leads to constraints on the parameters in the model.

4.1. The hermitian case

To analyze under which conditions there is a zero mode, we first consider the hermitian case, which is simpler. That is, we assume that $m \in \mathbb{R}$. We also write $t_1 = te^{i\phi_t}$, $t_2 = te^{-i\phi_t}$, $d_1 = de^{i\phi_d}$ and $d_2 = de^{-i\phi_d}$, with $t \geqslant 0, d \geqslant 0, 0 \leqslant \phi_t < 2\pi, 0 \leqslant \phi_d < 2\pi$ all real. We then have

$$x_{-,-} = \frac{-m/2 - \sqrt{d^2 + (m/2)^2 - t^2}}{t\cos\phi_t - \sqrt{d^2 - t^2\sin^2\phi_t}} \qquad x_{+,-} = \frac{-m/2 + \sqrt{d^2 + (m/2)^2 - t^2}}{t\cos\phi_t - \sqrt{d^2 - t^2\sin^2\phi_t}} \tag{24}$$

$$x_{-,+} = \frac{-m/2 - \sqrt{d^2 + (m/2)^2 - t^2}}{t\cos\phi_t + \sqrt{d^2 - t^2\sin^2\phi_t}} \qquad x_{+,+} = \frac{-m/2 + \sqrt{d^2 + (m/2)^2 - t^2}}{t\cos\phi_t + \sqrt{d^2 - t^2\sin^2\phi_t}}\ . \tag{25}$$

Analyzing the conditions that imply the existence of a zero mode (that is, either $|x_{-,-}| < 1$ and $|x_{+,-}| < 1$, or $|x_{-,+}| < 1$ and $|x_{+,+}| < 1$), we consider four different cases, determined by the expressions under the square roots being positive or negative. We find that it is necessary to have $d^2 > t^2\sin^2\phi_t$, while $d^2 + (m/2)^2 - t^2$ can have either sign. In addition, it is necessary that $m^2 < 4t^2\cos^2\phi_t$. Under these conditions, we have that $|x_{-,+}| < 1$ and $|x_{+,+}| < 1$ if $\cos\phi_t > 0$. If on the other hand $\cos\phi_t < 0$, we have that $|x_{-,-}| < 1$ and $|x_{+,-}| < 1$ instead. From this, we also find that it is necessary to have $\cos\phi_t \neq 0$. This condition is, however, already implied by $m^2 < 4t^2\cos^2\phi_t$. Summarizing, we find the following conditions in order that the system has a zero mode in the hermitian case

$$m^2 < 4t^2\cos^2\phi_t \qquad\qquad d^2 > t^2\sin^2\phi_t\ . \tag{26}$$

In the case of real hopping parameters, $\phi_t = 0, \pi$, this reduces to the well known conditions $|m| < 2|t|$ and $|d| > 0$ [66].

4.2. The general case

In the general case we have $x_{\pm,\pm} = \frac{-m \pm \sqrt{4d_1d_2 + m^2 - 4t_1t_2}}{(t_1+t_2) \pm \sqrt{4d_1d_2 + (t_1-t_2)^2}}$. To simplify the expressions (here and below), we introduce $D_2 = (d_1d_2 - t_1t_2)$, and put a factor $1/\sqrt{-4D_2}$ (which is in general complex) under the square roots. This of course might introduce an additional sign for the square root terms, but because we need simultaneous conditions for the different signs, this does influence the range of parameters for which there is a zero mode (however, the values of

the various $x_{\pm,\pm}$ might be swapped). With these caveats, we write

$$x_{\pm,\pm} = \frac{y_1 \pm \sqrt{y_1^2 - 1}}{y_2 \pm \sqrt{y_2^2 - 1}} \qquad y_1 = -\frac{m}{\sqrt{-4D_2}} \qquad y_2 = \frac{t_1 + t_2}{\sqrt{-4D_2}} \,. \tag{27}$$

We focus on the expression $y \pm \sqrt{y^2 - 1}$. Modulo the values at the branch cuts, we can write

$$y \pm \sqrt{y^2 - 1} = \begin{cases} e^{\pm i \arccos(y)} & \mathrm{Re}\,(y)\,\mathrm{Im}\,(y) > 0 \\ e^{\mp i \arccos(y)} & \mathrm{Re}\,(y)\,\mathrm{Im}\,(y) < 0 \,. \end{cases} \tag{28}$$

Because we are interested in the absolute values of $x_{\pm,\pm}$, we have to investigate $\mathrm{Im}(\arccos(y_1))$ and $\mathrm{Im}(\arccos(y_2))$. We demand that either $|x_{-,-}| < 1 \wedge |x_{+,-}| < 1$ or $|x_{-,+}| < 1 \wedge |x_{+,+}| < 1$. Analyzing these conditions, one finds that there is a zero mode when $|\mathrm{Im}(\arccos(y_1))| < |\mathrm{Im}(\arccos(y_2))|$, or in terms of the parameters of the model,

$$\left| \mathrm{Im}\left(\arccos\left(-\frac{m}{2\sqrt{t_1 t_2 - d_1 d_2}} \right) \right) \right| < \left| \mathrm{Im}\left(\arccos\left(\frac{t_1 + t_2}{2\sqrt{t_1 t_2 - d_1 d_2}} \right) \right) \right| . \tag{29}$$

We close this section by commenting on the case $d_1 d_2 = 0$. The criterion equation (29) is not in any way singular when $d_1 d_2 = 0$. However, we know that in this case, the model is closely related to the Hatano-Nelson model [90–92], see section 3. In particular, the eigenvalues for the finite size system are given by equation (17), showing that for generic parameters, the model does not have a zero mode for chains of finite size. However, equation (29) can certainly be satisfied when $d_1 d_2 = 0$. This means that the zero mode only occurs in the limit $L \to \infty$. We verified this behavior in the following way.

We first picked parameters, with $d_1 \neq 0$ and $d_2 = 0$, such that equation (29) is satisfied (i.e. there is a zero mode when $L \to \infty$). For a large, but finite system, the eigenvalues are given by equation (17), and generically, there are no eigenvalues that tend to zero when increasing the system size (which would be the case for a zero mode that is present already for finite system size). However, upon changing d_2 to a value such that $|d_2|$ is much smaller than the absolute values of all the other parameters in the system, the spectrum reorganizes itself in such a way that there is a zero mode that is present at finite system size. That is, there is a pair of eigenvalues that tends to zero upon increasing the system size.

In contrast to this, if we pick parameters with $d_1 \neq 0$ and $d_2 = 0$, such that equation (29) is not satisfied (i.e. there is no zero mode when $L \to \infty$), the spectrum only changes slightly, when slightly changing d_2 away from zero. In particular, no eigenvalues appear that tend to zero upon increasing the system size, in agreement with the absence of a zero mode.

5. Solution in the $L \to \infty$ limit

In section 3, we obtained a compact characterization of the eigenvalues for chains of arbitrary finite length, under the restriction that $t_1 = t_2$, but otherwise arbitrary complex parameters. Because obtaining the eigenvalues for large non-hermitian systems is often numerically unstable, we focus in this section on obtaining a compact characterization for the eigenvalues in the $L \to \infty$ limit. We do this for arbitrary complex parameters, so in this section we relax the constraint $t_1 = t_2$ that we imposed above. The result of this section is a complete characterization of the eigenvalues in terms of three polynomial equations, which can be solved numerically straightforwardly, without stability issues.

The starting point is the condition $\det(M) = 0$, where M is given by equation (10). Evaluating the determinant gives (after dropping a factor $(d_1 d_2 - t_1 t_2)^2$)

$$\begin{aligned}
&(a_1 - a_2)(a_3 - a_4)\left(x_1^{L+1} x_2^{L+1} + x_3^{L+1} x_4^{L+1}\right) \\
&-(a_1 - a_3)(a_2 - a_4)\left(x_1^{L+1} x_3^{L+1} + x_2^{L+1} x_4^{L+1}\right) \\
&+(a_1 - a_4)(a_2 - a_3)\left(x_1^{L+1} x_4^{L+1} + x_2^{L+1} x_3^{L+1}\right) = 0\,.
\end{aligned} \tag{30}$$

We recall that the (x_i, a_i) are determined by the bulk equations (7). To analyze this condition, we order the x_i according to their absolute values, $|x_1| \geqslant |x_2| \geqslant |x_3| \geqslant |x_4|$. From the bulk equation (8), it follows that $x_1 x_2 x_3 x_4 = 1$.

Generically, the condition equation (30) is dominated by $x_1^{L+1} x_2^{L+1}$. This means that we obtain the condition $(a_1 - a_2)(a_3 - a_4) = 0$. We find that, for generic parameters in the model, the only way in which one can have a double root for a is when $\lambda = 0$, i.e. in the case of a zero mode.

To show this, we need to analyze under which conditions there is a solution for which two values of a are identical, and check that they correspond to the solutions for x which are largest in absolute value. One can eliminate x from the bulk equations equations (7), giving rise to a fourth order polynomial in a, which we denote as $p_4(a)$. To find a double zero, one needs that $p_4(a)$ and $\frac{\mathrm{d}p_4(a)}{\mathrm{d}a}$ have a common zero. This in turn occurs when the *resultant* of $p_4(a)$ and $\frac{\mathrm{d}p_4(a)}{\mathrm{d}a}$ is zero, $\mathrm{Res}(p_4(a), \frac{\mathrm{d}p_4(a)}{\mathrm{d}a}) = 0$.

One can write $\mathrm{Res}(p_4(a), \frac{\mathrm{d}p_4(a)}{\mathrm{d}a}) = 16 d_1^4 d_2^2 \lambda^4 (t_1 + t_2)^4 (\lambda + m - t_1 - t_2)(\lambda + m + t_1 + t_2) f_8(\lambda)$, where $f_8(\lambda)$ is an eighth order polynomial in λ, which also depends on all the parameters in the model (the precise form of this polynomial is complicated, and not interesting for our purposes). We find that two values of a coincide for $d_1 d_2 = 0$, for $\lambda = 0$, for $t_2 = -t_1$ as well as for ten special values of λ that depend on the parameters of the model. These ten special values include $\lambda = -m \pm (t_1 + t_2)$. We do not consider these ten special values, because we are interested the generic eigenvalues of the model.

The case $d_1 d_2 = 0$ was treated in section 3. The case $\lambda = 0$, i.e. the zero modes, was analyzed in detail in section 4 above. In particular, we obtained a condition for the parameters in the model, such that there is an actual zero mode. This condition corresponded to the conditions $|x_1| > 1$ and $|x_2| > 1$. When there is no zero mode, we find the double solution for a actually corresponds to $a_3 = a_1$ or $a_4 = a_1$, so that equation (30) is not satisfied in the thermodynamic limit, despite the fact that there is a double solution for a.

When analyzing the case $t_2 = -t_1$, we come to the same conclusion, equation (30) is not satisfied in the thermodynamic limit, despite the fact that there is a double solution for a.

One is left to wonder how one can satisfy equation (30) when $\lambda \neq 0$ for arbitrary parameters? The answer is that we made an implicit assumption, namely we assumed that $|x_2| > |x_3|$, from which it followed that $x_1^{L+1} x_2^{L+1}$ dominates the expression. Under the condition that $|x_2| = |x_3|$, the condition equation (30) is dominated by more terms, such that solutions can be found for which $(a_1 - a_2)(a_3 - a_4) \neq 0$.

This observation allows us to obtain a rather compact representation of the eigenvalues λ in the limit of large system size, $L \to \infty$. Namely, we demand that two of the roots x_i of the bulk equation equation (8) have the same absolute value.

That is, we write

$$x_1 = \frac{s}{\kappa} \qquad x_2 = \kappa \mathrm{e}^{\mathrm{i}\alpha} \qquad x_3 = \kappa \mathrm{e}^{-\mathrm{i}\alpha} \qquad x_4 = \frac{1}{s\kappa}\,, \tag{31}$$

where κ and s are in general complex, while $0 \leqslant \alpha < 2\pi$ is real. Clearly $x_1x_2x_3x_4 = 1$, as required by the bulk equation (8).

The condition $x_1x_2x_3x_4 = 1$ is one of the Vieta equations, relating the roots of a polynomial to its coefficients [93]. Before continuing our analysis, we quickly explain the Vieta equations. For ease of presentation, we do this for a fourth order polynomial, as the generalization to the arbitrary case is clear. We write the polynomial in terms of its coefficients a_i and its roots r_j as follows

$$P(x) = a_4x^4 + a_3x^3 + a_2x^2 + a_1x + a_0 = a_4\prod_{j=1}^{4}(x - r_j) \ . \tag{32}$$

Expanding the right hand side, and comparing with the coefficients leads to the following equations

$$r_1 + r_2 + r_3 + r_4 = -a_3/a_4 \tag{33}$$
$$r_1r_2 + r_1r_3 + r_1r_4 + r_2r_3 + r_2r_4 + r_3r_4 = a_2/a_4 \tag{34}$$
$$r_1r_2r_3 + r_1r_2r_4 + r_1r_3r_4 + r_2r_3r_4 = -a_1/a_4 \tag{35}$$
$$r_1r_2r_3r_4 = a_0/a_4 \ . \tag{36}$$

These are the Vieta equations, which relate the coefficients of a polynomial to its roots. We note that the left hand sides correspond to the elementary symmetric polynomials evaluated at the roots of the original polynomial $P(x)$.

In the case at hand we have $a_0 = a_4$, leading to the fourth Vieta equation $x_1x_2x_3x_4 = 1$ as stated above. The remaning three Vieta equations for the roots can then be written (after taking a linear combination) as

$$\begin{aligned}
\left(\kappa + \frac{1}{\kappa}\right)\left[\left(s + \frac{1}{s}\right) + 2\cos\alpha\right] &= \frac{2m(t_1 + t_2)}{d_1d_2 - t_1t_2} \\
\left(\kappa - \frac{1}{\kappa}\right)\left[\left(s + \frac{1}{s}\right) - 2\cos\alpha\right] &= \frac{2\lambda(t_1 - t_2)}{d_1d_2 - t_1t_2} \\
\left(\kappa + \frac{1}{\kappa}\right)^2 + 2\cos\alpha\left(s + \frac{1}{s}\right) &= \frac{\lambda^2 - m^2 - (t_1 + t_2)^2}{d_1d_2 - t_1t_2} \ .
\end{aligned} \tag{37}$$

The curve(s) in the complex plane determined by the eigenvalues λ in the limit $L \to \infty$ are obtained by varying $0 \leqslant \alpha < 2\pi$ (we note that α plays the role of the momentum k in the periodic case). In principle, one can eliminate κ and s from the Vieta equations, to obtain an equation for λ in terms of α and the parameters of the model. This results in a forth order equation in λ^2, which is not insightful. In practise, if one wants to obtain the actual curve, one can simply solve the equations (37) numerically. It should be noted that not all solutions for λ correspond to actual eigenvalues. This is because it needs to be checked that the roots are ordered as $|x_1| \geqslant |x_2| = |x_3| \geqslant |x_4|$. There are two branches for which $|x_2| = |x_3| \geqslant |x_1|, |x_4|$ or $|x_1|, |x_4| \geqslant |x_2| = |x_3|$, which *do not* lead to actual eigenvalues. Thus, we need the solutions of the Vieta equations (37) such that $1/|s| \leqslant |\kappa|^2 \leqslant |s|$. Equivalently, one can instead require that $|s| \leqslant |\kappa|^2 \leqslant 1/|s|$. Despite the fact that there are two non-physical branches, that do not lead to actual eigenvalues of the model, these non-physical branches play an important role in explaining the geometry of the actual curves the eigenvalues lie on. Without the additional constraint that the roots need to satisfy $|x_1| \geqslant |x_2| = |x_3| \geqslant |x_4|$, one would obtain smooth curves for the eigenvalues in the complex plane. With the additional necessary constraint however, one finds

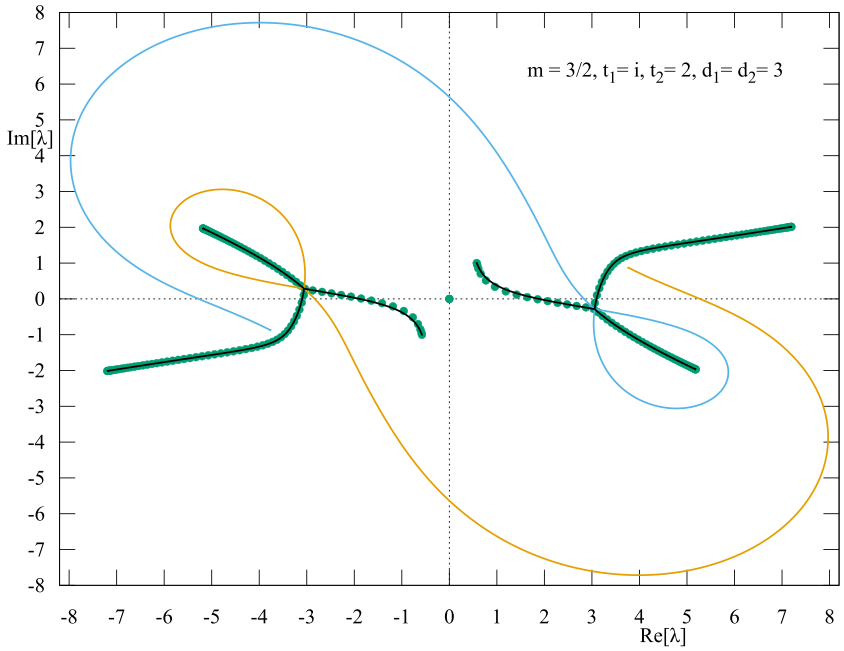

Figure 1. Plot for the non-hermitian Kitaev Chain with parameters $m = 3/2$, $t_1 = i$, $t_2 = 2$, $d_1 = d_2 = 3$. The black lines correspond to the eigenvalues of the infinite system. The blue and yellow lines correspond to solutions for λ of the Vieta equations, that do not correspond to actual eigenvalues of the model (as explained in the main text). The green dots correspond to eigenvalues of the finite system with $L = 100$.

that the actual curves on which the eigenvalues lie exhibit branching points. This is because these actual curves 'jump from one branch to another'.

To illustrate this, we plot the solutions for λ of the Vieta equations (37) for the parameters $m = 3/2$, $t_1 = i$, $t_2 = 2$ and $d_1 = d_2 = 3$ in figure 1. To generate the plot, we vary α over $0 \leqslant \alpha < 2\pi$ in steps of $2\pi/1000$. Using the solutions for κ and s, we determine in which way the absolute values of x_i are ordered. The black lines correspond to the ordering $|x_1| \geqslant |x_2| = |x_3| \geqslant |x_4|$, that is, to actual eigenvalues of the model. The blue and yellow lines correspond to the other two orderings, that do not lead to eigenvalues of the model. Finally, the green dots correspond to the eigenvalues of the finite chain with $L = 100$. Figure 1 clearly shows that the green dots closely follow the black lines, with only small deviations, caused by finite size effects. In addition, it is clear that the blue and yellow lines do not correspond to actual eigenvalues of the model. We also note the presence of the zero mode in the spectrum of the finite model. Zero modes do not correspond to solutions of the Vieta equations, as explained above.

The fact that the solutions for x come in three different 'branches', with only one corresponding to actual eigenvalues of the model, nicely explains the presence of the 'branching points' that are present in the spectra of the non-hermitian Kitaev chain. We show a more intricate example of this in section 7 below. There, we also discuss the known stability problems of finding the eigenvalues of a large finite (non-hermitian) system.

We close this section by noting that if we know the spectrum for a given set of parameters, we in fact know the spectrum for a one-parameter set of parameters. In particular, the right

hand sides of the Vieta equations (37) are invariant under

$$m \to m\mathrm{e}^{\mathrm{i}\,\phi} \qquad t_s \to t_s\mathrm{e}^{\mathrm{i}\,\phi} \qquad t_d \to t_d\mathrm{e}^{\mathrm{i}\,\phi} \qquad d_1 d_2 \to d_1 d_2 \mathrm{e}^{2i\,\phi} \qquad \lambda \to \lambda\mathrm{e}^{\mathrm{i}\,\phi}\,, \quad (38)$$

meaning that if one changes phases of the parameters in the way indicated, the whole spectrum is rigidly phase rotated. We note that this basically corresponds to multiplying the whole matrix equation (3) by a constant phase, which leaves the eigenvectors invariant (one can of course also rescale the spectrum in the same way).

6. Presence of the skin effect

Because we have a rather compact characterization of the eigenvalues of the model in the thermodynamic limit we can, in principle, analyze in detail for which parameters the model has a skin effect. Eigenvectors that exhibit skin effect are exponentially localized to the boundary of the systems. We determine the parameters for which the system exhibits a skin effect, and if so, to which eigenvectors this pertains (there can be cases where only a subset of eigenvectors exhibit skin effect).

In solving the model in the infinite size limit, we obtained that two roots of the bulk equation are equal in absolute value, see equation (31). Because the roots x_2 and x_3 with $|x_2| = |x_3|$ determine the corresponding eigenvector, we find that there is no skin effect when $|x_2| = |x_3| = 1$. The eigenvalues of the eigenstates that do not show a skin effect, lie on the curves of the eigenvalues in the periodic case $\lambda_{\pm}(k)$, as given by equation (11). We are interested in determining the parameters of the model, for which there are eigenstates that do not show the skin effect for extended ranges of k. We will not in general try to locate isolated points.

There is a long history of determining the location of the roots of polynomials in the complex plane. One of the main reasons for this, is that it is used extensively in system analysis, in particular for systems that are linear and time invariant. Such a system is stable, if the output is bounded, even in the limit when the evolved time goes to infinity. This is the case when all the roots of the characteristic polynomial corresponding to the system have negative real parts. Several algorithms exist to determine, how many roots have a negative real part, *without* having to determine the actual roots. Routh and Hurwitz independently developed such algorithms, leading to the Routh–Hurwitz stability criterion [94, 95], which determines if all the roots of a polynomial have negative real parts. One way to derive the criterion is to construct the sequence of Sturm polynomials associated with the polynomial under investigation [96].

The algorithm we focus on is tailored to determine the number of roots within, on and outside of the unit circle. This is achieved by using a conformal map, that maps the imaginary axis to the unit circle. In particular, the algorithm we use is due to Bistritz [97], but also in the case of finding the number of roots inside the unit circle, the topic has a long history, dating back a century at least [98].

For a polynomial with explicit coefficients, the algorithm fully determines the number of roots of each 'type'. We however, would like to determine the number of roots on the unit circle as a function of the parameters in the model. This is a harder problem, and although we believe we determined all cases for which there are at least two roots on the unit circle, we do not have a proof for this in the general case with complex parameters.

We do not repeat the full Bistritz algorithm here (which can be found in [97]), because it is a bit lengthy, and we do not need most of the details for our purposes. Therefor, we focus instead on the parts of the algorithm that are relevant for our analysis.

The starting point of the algorithm is a polynomial of degree n, $P_n(x)$, and we assume that $P_n(1) = 1$. As long as $P_n(1) \neq 0$, we can always rescale $P_n(x)$ as necessary. If $P_n(1) = 0$, we can factorize out the root $x = 1$. From the polynomial $P_n(x)$, a set of polynomials $T_i(x)$, of degree i with $i = n, n-1, \ldots, 0$ is constructed. In this paper, we do not describe the actual algorithm to determine the polynomials $T_i(x)$, but simply state the results and refer to [97] for the details.

In general, the algorithm to determine the polynomials $T_i(x)$ can be 'regular' or 'singular'. For now, we assume that the algorithm is 'regular' and discuss the singular case below. We assume that we obtained the polynomials $T_i(x)$ explicitly.

From the polynomials $T_i(x)$ one forms the sequence

$$A = \{T_n(1), T_{n-1}(1), \ldots T_1(1), T_0(1)\} \ . \tag{39}$$

The algorithm to define the $T_i(x)$ guarantees that $T_i(1)$ is real for all i. Therefore, we can define ν_n as the number of sign changes in the sequence A. The number of zeroes of $P(x)$ inside the unit circle is then given by $\alpha_n = n - \nu_n$, while the number of zeroes of $P(x)$ outside the unit circle is given by $\gamma_n = \nu_n$.

If the polynomial $P_n(x)$ has one or more roots on the unit circle, the algorithm is 'singular'. In particular, the algorithm is singular at level s if $T_s(0) \neq 0$ and $T_{s-1}(x) \equiv 0$. In this case, the algorithm proceeds in a slightly different manner, and one obtains different polynomials $T'_{s-1}(x), T'_{s-2}(x), \ldots T'_1(x), T'_0(x)$ (which also have the property that $T'_i(1)$ is real for all i). In this case, one defines

$$A = \left\{T_n(1), T_{n-1}(1), \ldots, T_s(1), T'_{s-1}(1), T'_{s-2}(1) \ldots T'_1(1), T'_0(1)\right\} \tag{40}$$

$$B = \left\{T_s(1), T'_{s-1}(1), T'_{s-2}(1) \ldots T'_1(1), T'_0(1)\right\} \ . \tag{41}$$

Again, ν_n is the number of sign changes in A, but we now also define ν_s as the number of sign changes in B. In this case, the number of zeroes inside the unit circle is $\alpha_n = n - \nu_n$, the number of zeroes on the unit circle is $\beta_n = 2\nu_s - s$, while the number of zeroes outside of the unit circle is $\gamma_n = n - \alpha_n - \beta_n$.

For our problem, we analyze the bulk equation, which we write as follows

$$P(x) = \frac{1}{N_2}\left(D_2\left(1 + x^4\right) + x^3\left(-\lambda t_d - m t_s\right) + x\left(\lambda t_d - m t_s\right) + x^2\left(N_2 + 2 m t_s - 2 D_2\right)\right) \ , \tag{42}$$

with

$$N_2 = \lambda^2 - (m + t_s)^2 \qquad D_2 = d_1 d_2 - t_1 t_2 \qquad t_s = t_1 + t_2 \qquad t_d = t_1 - t_2 \ . \tag{43}$$

The polynomial $P(x)$ is scaled such that $P(1) = 1$.

To proceed, we note that when the system does not exhibit skin effect, the eigenvalues λ of the *open chain* that we study lie on the curve given by the eigenvalues of the *periodic chain*. We use this information when analyzing the sequences A and B defined above. The eigenvalues for the periodic chain are given by equation (11) with $0 \leqslant k < 2\pi$.

Because the solution in the periodic case satisfies the same bulk equation, we find that $x = \mathrm{e}^{\mathrm{i}k}$ is a root of $P(x)$ provided that we set $\lambda = \lambda_+(k)$. Similarly, $x = \mathrm{e}^{-\mathrm{i}k}$ is a root of $P(x)$ for $\lambda = \lambda_-(k)$. In both cases, at least one of the roots lies on the unit circle, implying that the Bistritz algorithm is singular at some level (when λ is set to $\lambda_\pm(k)$). For this reason, we should analyze at which level the algorithm is singular, depending on the parameters of the model.

If we find that the algorithm is singular at level s, with s even, we know that the number of zeroes on the unit circle, given by $\beta_n = 2\nu_s - s$ is also even. This implies that there are at least two zeroes on the unit circle, because we know that there is at least one such zero. This in turn implies the absence of the skin effect. Because the product of the roots $x_1x_2x_3x_4 = 1$, we also know that is it not possible to have precisely three roots on the unit circle.

6.1. Skin effect for the model with real parameters

In the case of polynomials with complex parameters, the Bistritz algorithm becomes cumbersome, because constructing the polynomials $T_i(x)$ involves taking the complex conjugate. Therefore, we initially focus on the case with real parameters m, t_1, t_2, d_1, d_2, but of course allow λ, and hence N_2, to be complex. In this case, we obtain the following results for the polynomials $T_i(x)$. For $T_4(x)$, we have

$$\begin{aligned} T_4(x) &= 2\left(D_2\,\mathrm{Re}(N_2)\left(1-2x^2+x^4\right) - mt_s\,\mathrm{Re}(N_2)\left(x-2x^2+x^3\right)\right. \\ &\quad \left. +\mathrm{i}\,t_d\,\mathrm{Im}(\lambda N_2^*)\left(x-x^3\right)\right)/(N_2N_2^*) + 2x^2 \\ T_4(1) &= 2 \\ T_4(0) &= 2D_2\,\mathrm{Re}(N_2)/(N_2N_2^*)\ . \end{aligned} \tag{44}$$

For $T_3(x)$, we have

$$\begin{aligned} T_3(x) &= 2\left(\mathrm{i}D_2\,\mathrm{Im}(N_2)\left(1+x-x^2-x^3\right) - \mathrm{i}mt_s\,\mathrm{Im}(N_2)\left(x-x^2\right)\right. \\ &\quad \left. -t_d\,\mathrm{Re}(\lambda N_2^*)\left(x+x^2\right)\right)/(N_2N_2^*) \\ T_3(1) &= -4\,\mathrm{Re}(\lambda N_2^*)/(N_2N_2^*) \\ T_3(0) &= 2\mathrm{i}D_2\,\mathrm{Im}(N_2)/(N_2N_2^*)\ . \end{aligned} \tag{45}$$

For $T_2(x)$, we have

$$\begin{aligned} T_2(x) &= -2t_d\,\mathrm{Re}(\lambda)\left(1-x^2\right)/(\mathrm{i}\,\mathrm{Im}(N_2)) - 2x \\ T_2(1) &= -2 \\ T_2(0) &= -2t_d\,\mathrm{Re}(\lambda)/(\mathrm{i}\,\mathrm{Im}(N_2))\ . \end{aligned} \tag{46}$$

Finally, for $T_1(x)$, we have

$$\begin{aligned} N_2N_2^*\,T_1(x) &= 2\left(-D_2\,\mathrm{Im}(N_2)^2/(t_d\,\mathrm{Re}(\lambda)) + t_d\,\mathrm{Re}(\lambda N_2^*)\right)(1+x) + 2\mathrm{i}mt_s\,\mathrm{Im}(N_2)(1-x) \\ N_2N_2^*\,T_1(1) &= -4D_2\,\mathrm{Im}(N_2)^2/(t_d\,\mathrm{Re}(\lambda)) + 4t_d\,\mathrm{Re}(\lambda N_2^*) \\ N_2N_2^*\,T_1(0) &= -2D_2\,\mathrm{Im}(N_2)^2/(t_d\,\mathrm{Re}(\lambda)) + 2t_d\,\mathrm{Re}(\lambda N_2^*) + 2\mathrm{i}mt_s\,\mathrm{Im}(N_2)\ . \end{aligned} \tag{47}$$

We do not explicitly state the constant T_0, because it is a long expression and we do not need it for our purposes.

We start by analyzing under which conditions $T_3(x) \equiv 0$. This requires $N_2 = N_2^*$ and $(\lambda + \lambda^*)t_d = 0$. The first condition $N_2 = N_2^*$ is equivalent to $\mathrm{Re}(\lambda) = 0$ or $\mathrm{Im}(\lambda) = 0$. The second condition $(\lambda + \lambda^*)t_d = 0$ is equivalent to $\mathrm{Re}(\lambda) = 0$ or $t_d = 0$. Combined, we find that $T_3(x) \equiv 0$ requires that either $\mathrm{Re}(\lambda) = 0$ or that $\mathrm{Im}(\lambda) = t_d = 0$.

We remark that $\mathrm{Re}(\lambda) = 0$ implies that $4d_1d_2\sin(k)^2 + (m + (t_1+t_2)\cos(k))^2 \leqslant 0$, which can only occur if d_1 and d_2 have opposite signs (or when $d_1d_2 = 0$). On the other hand, if $\mathrm{Im}(\lambda) = 0$ and $t_d = 0$ we need $4d_1d_2\sin(k)^2 + (m + (t_1+t_2)\cos(k))^2 \geqslant 0$.

Table 1. Absence of the skin effect, in the case of real parameters.

condition on parameters	condition on k
$m=0$	$\forall k$
$t_1=t_2$	$\forall k$
$t_2=-t_2$	$\forall k$
$d_1d_2<0$	$4d_1d_2\sin(k)^2+(m+(t_1+t_2)\cos(k))^2<0$

Finally, we note that the explicit form of $\lambda_\pm(k)$ implies that for $t_d=0$, we have that either $\mathrm{Re}(\lambda)=0$ or $\mathrm{Im}(\lambda)=0$. Hence, for $t_d=0$ the algorithm is singular at level $s=4$ (we recall that we assumed that all the parameters of the model are real). This finishes the analysis of the conditions $T_3(x)\equiv 0$.

The other way in which we can have two roots on the unit circle is when the algorithm is singular at level 2, that is when $T_1(x)\equiv 0$ (and $T_2(0)\neq 0$). By analyzing the form of $T_1(x)$, making use of the explicit form of the eigenvalues in the periodic case $\lambda_\pm(k)$, one finds that $T_1(x)\propto mt_st_d$. Because $T_2(0)\neq 0$ for $m=0$ or $t_s=0$, we obtain that the algoritm is also singular when either $m=0$ or $t_s=0$.

We summarize the result in table 1. For the model with real parameters, there is no skin effect when either $m=0$, or when $t_1=\pm t_2$. In addition, there is no skin effect when $\mathrm{Re}(\lambda)=0$, which occurs (over an extended range for k) when $4d_1d_2\sin(k)^2+(m+(t_1+t_2)\cos(k))^2<0$, requiring $d_1d_2<0$ (we note that $|d_1d_2|$ should be sufficiently large in order to have $4d_1d_2\sin(k)^2+(m+(t_1+t_2)\cos(k))^2<0$). We note that the eigenvalues being real ($\mathrm{Im}(\lambda)=0$) alone does not imply that the skin effect is absent. Real eigenvalues can have skin effect when $t_1\neq t_2$.

To illustrate these results, we plot the (complex) spectrum of the model for several parameters. In all the plots, we use the following color conventions. The gray curves represent the eigenvalues of the model with *periodic* boundary conditions. The green dots represent the eigenvalues of the open chain of finite length with $L=100$ sites. The blue lines represent eigenvalues of the infinite open chain, corresponding to eigenstates that *do* have skin effect. Finally, the red lines represent eigenvalues of the infinite open chain, corresponding to eigenstates that *do not* have skin effect. The latter eigenvalues also correspond to eigenvalues of the periodic chain.

In figure 2, we plot the eigenvalues of the system with parameters $m=2/5$, $t_1=2$, $t_2=1$, $d_1=-d_2=\sqrt{3}$. The figure clearly shows that for these parameters (which do no fall in one of the classes $m=0$ or $t_1=\pm t_2$), some of the eigenstates of the infinite open chain do show skin effect, while others do not. The eigenvalues that are purely imaginary do not show skin effect, while those that lie in the region bounded by the two ovals (corresponding to eigenvalues of the periodic case) do show skin effect. Interestingly, there are real (non-zero) eigenvalues that correspond to states that do exhibit skin effect. In the hermitian case, non-zero (and necessarily real) eigenvalues do not exhibit skin effect. In figure 3, we plot the absolute value of the eigenstate coefficients as a function of position for two eigenvalues of the finite chain namely $\lambda\approx 3.0182$ in the left panel (a) (real eigenvalue with skin effect, using a logarithmic scale) and $\lambda\approx 4.3949i$ in the right panel (b) (purely imaginary eigenvalue without skin effect). In particular, in the left panel of figure 3, we find that the structure of the eigenvector is an exponentially damped oscillation. The exponential decay signifies the presence of the skin effect. In terms of the non-Bloch band theory of non-hermitian systems introduced in [60], the eigenvectors that do not exhibit skin effect have a β parameter such that $|\beta|=1$ (or a real momentum), while the eigenvectors that do exhibit skin effect have a β parameter such that $|\beta|\neq 1$ (i.e. its 'momentum' is complex).

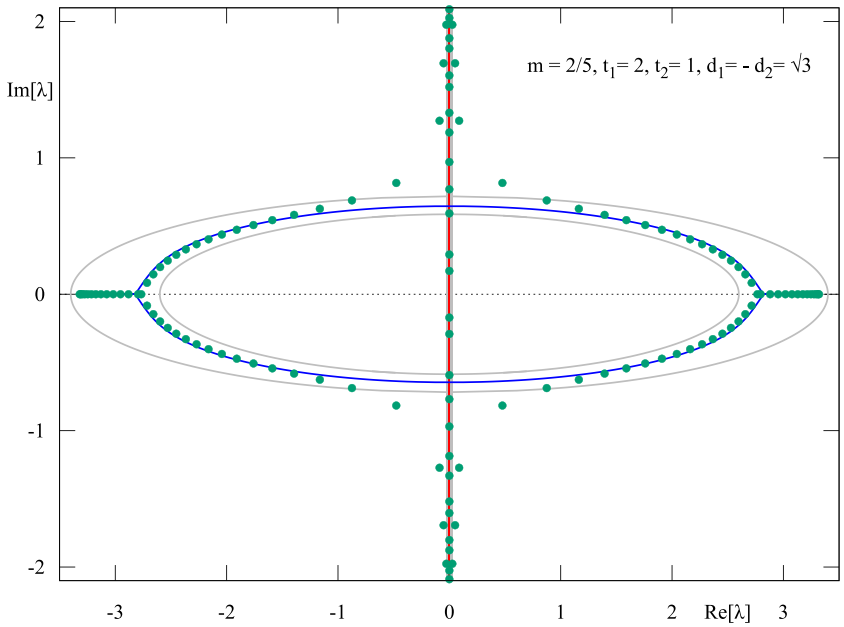

Figure 2. The eigenvalues of the model with parameters $m = 2/5$, $t_1 = 2$, $t_2 = 1$, $d_1 = -d_2 = \sqrt{3}$. The gray lines correspond to the periodic case; the green dots correspond to the open finite chain with $L = 100$; the blue (red) lines correspond eigenvalues of the open infinite chain whose eigenstates do (do not) exhibit the skin effect. The eigenvalues along the imaginary axis extent to $\lambda \approx \pm 4.4495i$.

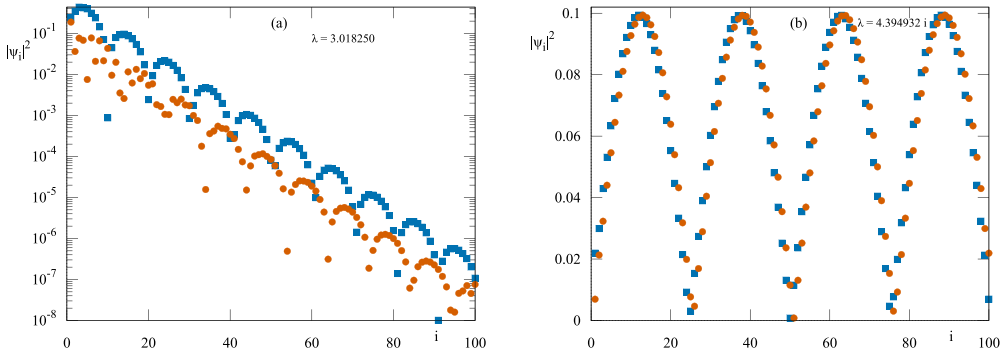

Figure 3. The amplitude of eigenstate coefficients $|\psi_i|^2$ as a function of the site index i for two states of the finite $L = 100$ model with parameters $m = 2/5$, $t_1 = 2$, $t_2 = 1$, $d_1 = -d_2 = \sqrt{3}$. The blue squares (orange dots) correspond to the first (second) component of the eigenvector of a given site i. The left panel (a) corresponds to a real eigenvalue ($\lambda \approx 3.0182$) showing skin effect (note the logarithmic scale), the right panel (b) corresponds to a purely imaginary eigenvalue ($\lambda \approx 4.3949i$) without skin effect.

Depending on the parameters, it can also happen that either all the eigenstates of the model have skin effect (this is the generic case), or none of the eigenstates have skin effect. In figure 4, we show an example of either case.

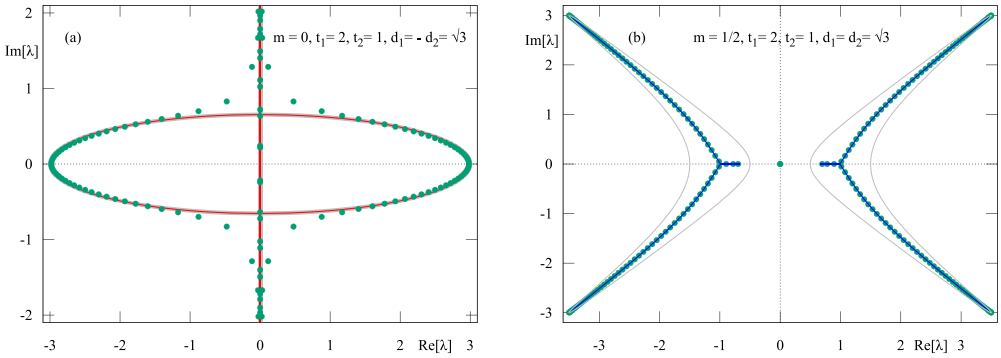

Figure 4. The eigenvalues for two sets of parameters. The color coding is the same as in figure 2. The parameters for the left panel (a) are $m=0$, $t_1=2$, $t_2=1$, $d_1=-d_2=\sqrt{3}$; in this case, none of the eigenstates exhibit skin effect, thus the red and gray curves coincide. The purely imaginary eigenvalues extend to $\pm(1+2\sqrt{3})i \approx \pm 4.4641i$. We cut off the figure for clarity. The parameters for the right panel (b) are $m=1/2$, $t_1=2$, $t_2=1$, $d_1=d_2=\sqrt{3}$; in this case, all the eigenstate exhibit skin effect. We note that in this case, there is zero-mode.

6.2. Skin effect for the model with complex parameters

In this section, we consider the model with complex parameters, generalizing the results of the previous section. As in the case of real parameters, we do not try to find all isolated points for which the eigenstates do not show a skin effect (this could occur when the curves describing the eigenvalues in the periodic case, i.e. $\lambda_\pm(k)$, self intersect).

In the previous section, we obtained that $m=0$, $t_1=t_2$ and $t_1=-t_2$ are three different sufficient conditions implying that there is no skin effect for all the eigenstates in the case of real parameters. We now argue that these three conditions remain sufficient in the case of complex parameters.

To show this, we consider the Vieta equations (37), and solve them for κ, s and λ under the conditions $m=0$, $t_1=-t_2$ or $t_1=t_2$. When either $m=0$ or $t_1=-t_2$, we find that there are solutions with $\kappa=\pm i$. When $t_1=t_2$, there are solutions with $\kappa=\pm 1$. Because in all these cases, $|\kappa|=1$ we find that the ordering of the roots satisfies $|x_1|\geqslant|x_2|=|x_3|\geqslant|x_4|$, which shows that the obtained solutions correspond to actual eigenvalues of the model. Because $|\kappa|=1$, the eigenstates do not exhibit a skin effect. Indeed, in these cases the form of λ as obtained from the Vieta equations corresponds to the eigenvalues of the periodic case, $\lambda_\pm(k)$, which has to be true in the absence of the skin effect.

We continue by generalizing the results for real parameters, that originated from the condition $T_3(x)\equiv 0$. In order to do this, we need the form of the Bistritz polynomials for complex parameters. Because these are quite involved, we state them in the appendix. In particular, we need $T_3(x)$ as given in equation (A2).

We find that the condition $T_3(x)\equiv 0$ is equivalent to the following conditions on the parameters in the model

$$\mathrm{Im}\,(D_2N_2^*)=0 \qquad \mathrm{Im}\,(mt_sN_2^*)=0 \qquad \mathrm{Re}\,(\lambda t_dN_2^*)=0\,. \tag{48}$$

Let us denote the argument of m, t_s, etc by ϕ_m, ϕ_{t_s}, etc then the conditions above reduce to

$$\phi_{D_2}=\phi_{N_2} \bmod \pi \qquad \phi_m+\phi_{t_s}=\phi_{N_2} \bmod \pi \qquad \phi_\lambda+\phi_{t_d}=\phi_{N_2}+\pi/2 \bmod \pi\,. \tag{49}$$

Table 2. Sufficient conditions for absence of the skin effect (due to $T_3(x) \equiv 0$).

t_s	t_d	m	$d_1 d_2$	λ	absence skin effect
$\lvert t_s\rvert e^{i\phi_{t_s}}$	$\pm i\lvert t_d\rvert e^{i\phi_{t_s}}$	$\pm\lvert m\rvert e^{i\phi_{t_s}}$	$+\lvert d_1 d_2\rvert e^{2i\phi_{t_s}}$	$\pm\lvert\lambda\rvert e^{i\phi_{t_s}}$	$\forall k$
$\lvert t_s\rvert e^{i\phi_{t_s}}$	$\pm i\lvert t_d\rvert e^{i\phi_{t_s}}$	$\pm\lvert m\rvert e^{i\phi_{t_s}}$	$-\lvert d_1 d_2\rvert e^{2i\phi_{t_s}}$	$\pm\lvert\lambda\rvert e^{i\phi_{t_s}}$	$-4\lvert d_1 d_2\rvert \sin(k)^2 + (\pm\lvert m\rvert + \lvert t_s\rvert\cos(k))^2 > 0$
$\lvert t_s\rvert e^{i\phi_{t_s}}$	$\pm\lvert t_d\rvert e^{i\phi_{t_s}}$	$\pm\lvert m\rvert e^{i\phi_{t_s}}$	$-\lvert d_1 d_2\rvert e^{2i\phi_{t_s}}$	$\pm i\lvert\lambda\rvert e^{i\phi_{t_s}}$	$-4\lvert d_1 d_2\rvert \sin(k)^2 + (\pm\lvert m\rvert + \lvert t_s\rvert\cos(k))^2 < 0$

We note that N_2 is not independent of the parameters. Making use of the explicit form of λ in the periodic case, we obtain

$$N_2 = \lambda^2 - (m + t_s)^2 = 2mt_s(\cos(k) - 1) + 4D_2 \sin(k)^2 + 2i\lambda t_d \sin(k) \ , \quad (50)$$

which implies that the relations equation (49) are satisfied, provided that $\phi_{D_2} = \phi_m + \phi_{t_s} = \phi_\lambda + \phi_{t_d} + \pi/2 \bmod \pi$. To continue, we assume that $\phi_m = \phi_{D_2} - \phi_{t_s} \bmod \pi$ and $\phi_\lambda = \phi_{D_2} - \phi_{t_d} - \pi/2 \bmod \pi$. Then, the condition $T_3(x) \equiv 0$ reduces to

$$|\lambda|^2 \sin(\phi_{D_2} - 2\phi_{t_d}) + \left(|m|^2 - |t_s|^2\right) \sin(\phi_{D_2} - 2\phi_{t_s}) = 0 \ . \quad (51)$$

Because we are interested in extended regions in k for which there is no skin effect, we obtain that $\phi_{t_d} = \phi_{t_s} \bmod \pi/2$, and $\phi_{D_2} = 2\phi_{t_s} = 2\phi_{t_d} \bmod \pi$. Because of the relation $D_2 = d_1 d_2 - t_1 t_2$, we can replace the relation $\phi_{D_2} = 2\phi_{t_s} \bmod \pi$ by $\phi_{d_1 d_2} = 2\phi_{t_s} \bmod \pi$, where $\phi_{d_1 d_2}$ is the phase of $d_1 d_2$.

Combined, we find the following conditions, which are necessary in order that the Bistritz algorithm is singular at level 4

$$\phi_m = \phi_{t_s} \bmod \pi \quad \phi_\lambda = \phi_{t_d} + \pi/2 \bmod \pi \quad \phi_{d_1 d_2} = 2\phi_{t_s} \bmod \pi \quad \phi_{t_d} = \phi_{t_s} \bmod \pi/2 \ . \quad (52)$$

We still need to check when these conditions are compatible with the explicit form of the eigenvalues in the periodic case, $\lambda_\pm(k)$ as given in equation (11). By analyzing the form of $\lambda_\pm(k)$, taking the phase relations into account, one finds that the form of $d_1 d_2$ is crucial. Generically, we write $d_1 d_2 = |d_1 d_2| e^{i\phi_{d_1 d_2}}$. In table 2, we state the conditions such that the eigenstates do not show a skin effect (due to $T_3(x) \equiv 0$), resulting from this analysis. We note that the third line also follows from the analysis of the case with real parameters in the previous subsection and the result that phase-rotating the parameters of the model according to equation (38) leads to a rigid phase rotation of the spectrum.

An obvious check on these results is to consider the hermitian case, with $N_2, \lambda, m, D_2, t_s$ all real, and t_d purely imaginary. In this case, one finds that indeed $T_3(x) \equiv 0$ implying that the Bistritz algorithm is singular at level 4. This in turn implies that the eigenstates do not have a skin effect, as expected.

The other way in which the skin effect is absent, is when $T_1(x) \equiv 0$. The coefficients of the polynomial $T_1(x)$ are much more involved, see equation (A4). We therefore do not attempt to fully characterize for which (complex) parameters of the model one has $T_1(x) \equiv 0$. However, above we argued based on the Vieta equations that for either $m = 0$, $t_s = 0$, or $t_d = 0$, the eigenstates do not show a skin effect. This means that under these conditions $T_1(x) \equiv 0$ even when the other parameters are complex. We are interested in generic results, that is, extended regions of the curves of eigenvalues, for which the skin effect is absent. We believe that the conditions provided, exhaust all these cases. The argument in favor of this statement is that we need that $T_1(x) \equiv 0$ with $\lambda = \lambda_\pm(k)$, for an extended range of k. Due to the form of $\lambda_\pm(k)$, this only

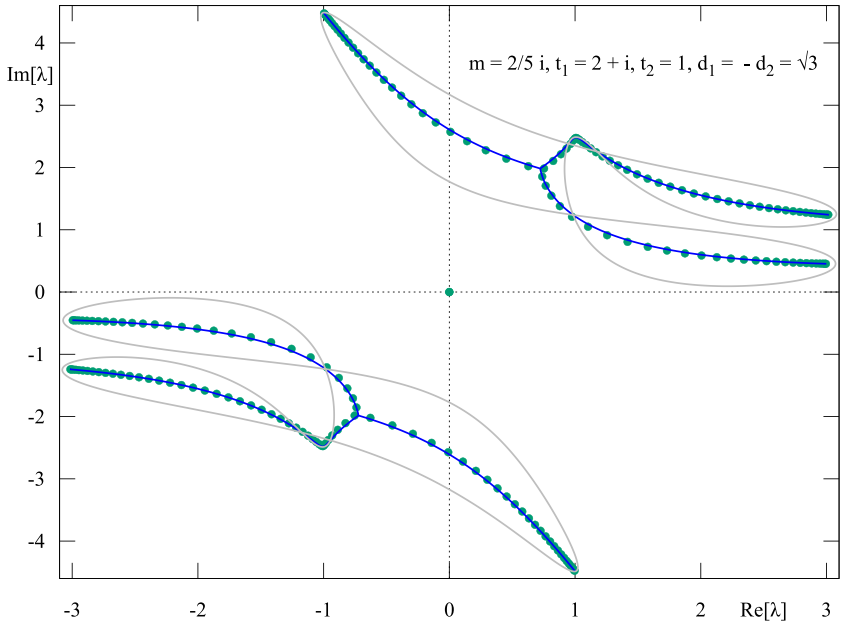

Figure 5. The eigenvalues for a set including complex parameters, namely $m = 2i/5$, $t_1 = 2 + i$, $t_2 = 1$, $d_1 = -d_2 = \sqrt{3}$. The color coding is the same as in figure 2.

seems possible when the various terms of $\lambda_\pm(k)$ have the same argument, or when one or more of the parameters is zero.

We conclude this section with a characteristic example of the eigenvalues for a case with complex parameters, namely $m = 2i/5, t_1 = 2 + i, t_2 = 1, d_1 = -d_2 = \sqrt{3}$ as shown in figure 5. In this generic case, all the generic eigenstates exhibit the skin effect. As expected, the spectrum is significantly more complex compared to the cases we showed with real parameters. We note that the gray curves of the eigenvalues $\lambda_\pm(k)$ in the periodic case intersect themselves. The eigenvalues of the open chain in the large system size limit (given by the blue curves) cross these intersection points. This means that the eigenstates corresponding to these (six) special eigenvalues do not have a skin effect. We checked this behavior explicitly, by solving the bulk equation (8), confirming that two solutions for x indeed have modulus one. In addition, we checked that the Bistritz polynomial $T_1(x) \equiv 0$ for the given parameters and the eigenvalue λ.

7. Analysis of an example

We studied the non-hermitian Kitaev chain for general complex parameters, pushing analytical methods as far as possible. We now summarize our results, by means of an example. We use the chain with parameters $m = 2/5$, $t_1 = 2 + i$, $t_2 = 1$, $d_1 = -d_2 = \sqrt{3}$ for this purpose. One of the main results we obtained in this paper, is the characterization of the eigenvalues of the infinite size system, in terms of three Vieta equations (37), for λ which we repeat here for convenience,

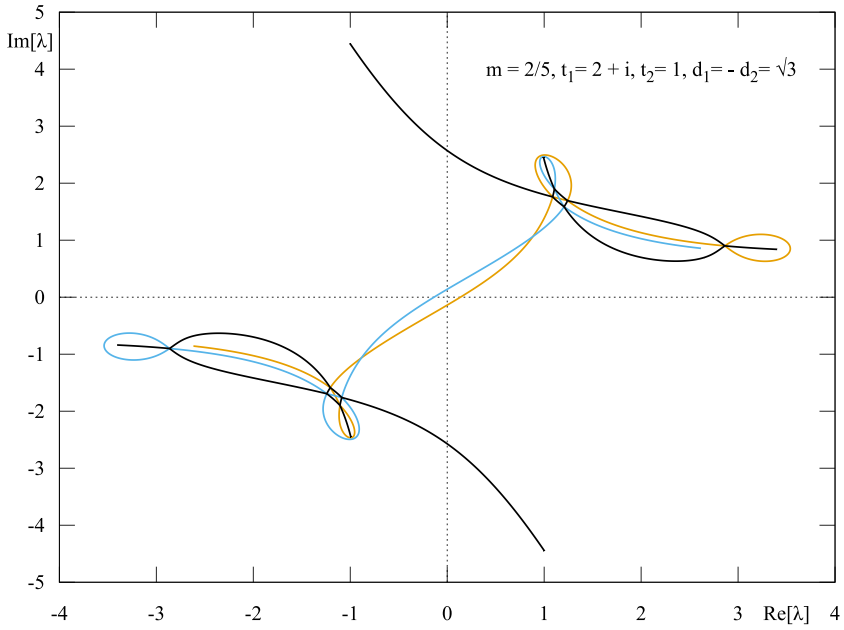

Figure 6. Solutions for λ of the Vieta equations, for $m = 2/5$, $t_1 = 2+i$, $t_2 = 1$, $d_1 = -d_2 = \sqrt{3}$. Only the black lines correspond to actual eigenvalues. For the blue and dark-yellow lines, the solutions x_i of the bulk equation correspond to one of the branches that do not correspond to actual eigenvalues.

$$\begin{aligned}
\left(\kappa+\frac{1}{\kappa}\right)\left[\left(s+\frac{1}{s}\right)+2\cos\alpha\right] &= \frac{2m\,(t_1+t_2)}{d_1d_2-t_1t_2}\\
\left(\kappa-\frac{1}{\kappa}\right)\left[\left(s+\frac{1}{s}\right)-2\cos\alpha\right] &= \frac{2\lambda\,(t_1-t_2)}{d_1d_2-t_1t_2}\\
\left(\kappa+\frac{1}{\kappa}\right)^2+2\cos\alpha\left(s+\frac{1}{s}\right) &= \frac{\lambda^2-m^2-(t_1+t_2)^2}{d_1d_2-t_1t_2}\,.
\end{aligned} \tag{53}$$

where κ and s are in general complex. The eigenvalue curves λ are obtained by varying $0 \leqslant \alpha < 2\pi$, and obtaining the solution of the three Vieta equations (37). *A priori*, the solutions of these equations are continuous and smooth as a function of the parameter α. Importantly, only those λ that correspond to solutions that satisfy $1/|s| \leqslant |\kappa|^2 \leqslant |s|$ are actual eigenvalues of the model as explained in section 5. This explains the observed branched structure of the actual eigenvalues.

In figure 6, we show the eigenvalues of the model with parameters $m = 2/5$, $t_1 = 2+i$, $t_2 = 1$, $d_1 = -d_2 = \sqrt{3}$ as an illustration. The actual eigenvalues (the black lines) form a rather intricate pattern, which can be explained in terms of the three different branches of solutions of the Vieta equations. Figure 6 also shows the other two branches (the blue and yellow lines), that do not correspond to eigenvalues of the model. It is interesting to note the regions where the black lines 'intersect'. Here, the eigenvalues do not cross, nor do they repel, but form a rhombic structure.

We saw that having a concise characterization of the eigenvalues of the infinite system size explains the structure of the curves the eigenvalues lie on. There is another reason why having a concise characterization for the infinite system size model is useful, apart from that its

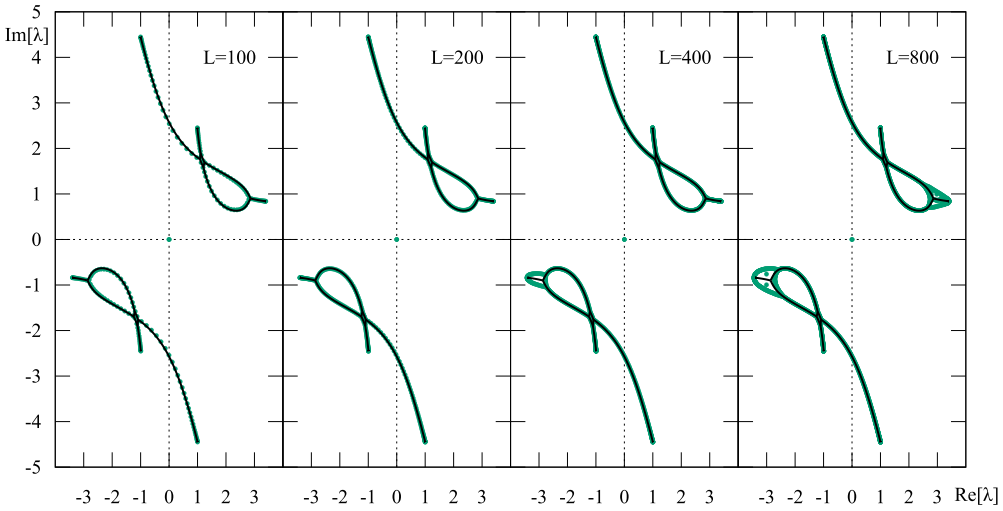

Figure 7. Finite size eigenvalues λ for the model with parameters $m = 2/5$, $t_1 = 2 + i$, $t_2 = 1$, $d_1 = -d_2 = \sqrt{3}$. The black lines correspond to actual eigenvalues in the limit $L \to \infty$. The different panels show the numerically obtained eigenvalues (using machine precision) for the sizes $L = 100$, $L = 200$, $L = 400$ and $L = 800$, showing the instability of the algorithm (green dots).

interesting in its own right. Namely, as is well known, obtaining the eigenvalues for large, non-hermitian systems showing skin-effect is often numerically unstable. We illustrate this using the same example, by plotting the eigenvalues, as obtained using *machine precision* denationalization for system sizes $L = 100$, $L = 200$, $L = 400$ and $L = 800$. The results are shown in figure 7 as the green dots, together with the infinite system size results.

We clearly see that for sizes $L = 100$ and $L = 200$, the eigenvalues closely follow the black lines corresponding to the infinite size model, with only minor difference due to the finite size effects. However, already for $L = 400$, there is a region where the finite size eigenvalues deviate substantially from curves for infinite size. Moreover, the 'eigenvalues' in this region do not satisfy particle-hole symmetry (dictating that if λ is an eigenvalue, so is $-\lambda$), which clearly indicates that these values obtained by the denationalization algorithm are incorrect. For $L = 800$, the situation gets worse. In principle, one can obtain the correct eigenvalues even for these larger system sizes, if one uses a denationalization algorithm employing higher precision arithmetic, but in practise, this will be much slower that obtaining the infinite system size results.

By making use of the exact solution, we studied the presence of the skin effect. There exist methods to determine if a model exhibits skin effect for a given set of parameters. Here, we also characterize which eigenvalues have eigenstates showing the skin effect, or rather, which ones do not show skin effect. We formulated this condition in terms of the solutions for x of the bulk equation (7), namely if at least two (out of the four) solutions lie on the unit circle, the corresponding eigenstate does not have a skin effect. We used the Bistritz algorithm to determine under which conditions there are states without skin effect, and to which eigenvalues these correspond. We provided a full characterization for the non-hermitian model with real

parameters. For the general model with complex parameters we provide sufficient conditions for the absence of the skin effect, which we believe are also necessary.

Finally, we studied under which conditions, the non-hermitian Kitaev chain has a zero mode (for the hermitian Kitaev chain, this corresponds to the region where the model is in the topological phase). It turns out that this region has perhaps a more complicated structure than one would expect. Namely, the model has a zero mode when the following condition is satisfied,

$$\left|\mathrm{Im}\left(\arccos\left(-\frac{m}{2\sqrt{t_1t_2-d_1d_2}}\right)\right)\right| < \left|\mathrm{Im}\left(\arccos\left(\frac{t_1+t_2}{2\sqrt{t_1t_2-d_1d_2}}\right)\right)\right| . \tag{54}$$

At the boundary of this region, the model is gapless, but even outside of this region, the model can be gapless. In the hermitian version of the model, this would correspond to a metallic, gapless system.

8. Discussion

We studied the non-hermitian Kitaev model for arbitrary, complex parameters. By using a novel method, we obtained a concise characterization of the eigenvalues in the thermodynamic limit for arbitrary complex parameters. Using this method, we explained the branched structure of the eigenvalues in the complex plane. In addition, we used the solution to obtain for which parameters, the model exhibit a skin effect, and if so, to which eigenvalues this pertains. For real parameters, we obtained this in full, while for arbitrary complex parameters, we obtained sufficient conditions, which we believe are also necessary. We fully characterized the parameters for which the model exhibits a zero mode. Finally, we discussed the stability issues that arise when one tries to numerically obtain the eigenvalues for large systems.

Despite the fact that non-hermitian one-dimensional models have been studied in great detail, it would be interesting to apply our method to characterize the eigenvalues in the thermodynamic limit to other, more complicated systems. One direct extension of the model we consider here, is to add terms that interpolate between open and periodic boundary conditions. Considering different models, one can think of systens with larger unit cells and/or longer range interactions. Obviously, this will lead to higher order equations and more complicated expressions.

Data availability statement

No new data were created or analysed in this study.

Appendix. Bistritz polynomials for complex parameters

In this appendix, we give the Bistritz polynomials $T_i(x)$ (with $4 \geqslant i \geqslant 1$) in the general case, that is for complex parameters. These results generalise the Bistritz polynomials given in section 6 for real parameters (and complex eigenvalues λ). We refer to that section for more details. More details on the Bistritz algorithm can be found in [97].

For arbitrary complex parameters and eigenvalue λ, the polynomial $T_4(x)$ reads

$$\begin{aligned}
T_4(x) &= 2\left(\mathrm{Re}\left(D_2N_2^*\right)\left(1-2x^2+x^4\right)+\mathrm{i}\,\mathrm{Im}\left(\lambda t_dN_2^*\right)\left(x-x^3\right)\right.\\
&\quad\left.-\mathrm{Re}\left(mt_sN_2^*\right)\left(x-2x^2+x^3\right)\right)/\left(N_2N_2^*\right)+2x^2\\
T_4(1) &= 2\\
T_4(0) &= 2\,\mathrm{Re}\left(D_2N_2^*\right)/\left(N_2N_2^*\right)\ .
\end{aligned}\tag{A1}$$

For $T_3(x)$, we obtain the following expression

$$\begin{aligned}
T_3(x) &= 2\left(-\mathrm{i}\,\mathrm{Im}\left(D_2N_2^*\right)\left(1+x-x^2-x^3\right)+\mathrm{i}\,\mathrm{Im}\left(mt_sN_2^*\right)\left(x-x^2\right)\right.\\
&\quad\left.-\mathrm{Re}\left(\lambda t_dN_2^*\right)\left(x+x^2\right)\right)/\left(N_2N_2^*\right)\\
T_3(1) &= -4\,\mathrm{Re}\left(\lambda t_dN_2^*\right)/\left(N_2N_2^*\right)\\
T_3(0) &= -2\mathrm{i}\,\mathrm{Im}\left(D_2N_2^*\right)/\left(N_2N_2^*\right)\ .
\end{aligned}\tag{A2}$$

$T_2(x)$ is given by

$$\begin{aligned}
T_2(x) &= 2\left(\mathrm{Re}\left(\lambda t_dD_2^*\right)\left(1-x^2\right)-\mathrm{i}\,\mathrm{Im}\left(mt_sD_2^*\right)\left(1-2x+x^2\right)\right)/\left(\mathrm{i}\,\mathrm{Im}\left(D_2N_2^*\right)\right)-2x\\
T_2(1) &= -2\\
T_2(0) &= 2\left(\mathrm{Re}\left(\lambda t_dD_2^*\right)-\mathrm{i}\,\mathrm{Im}\left(mt_sD_2^*\right)\right)/\left(\mathrm{i}\,\mathrm{Im}\left(D_2N_2^*\right)\right)\ .
\end{aligned}\tag{A3}$$

Finally, $T_1(x)$ is given by

$$\begin{aligned}
N_2N_2^*T_1(1) &= 2(1+x)\left[\mathrm{Re}\left(\lambda t_dN_2^*\right)-\frac{\mathrm{Im}\left(N_2D_2^*\right)^2\mathrm{Re}\left(\lambda t_dD_2^*\right)}{\mathrm{Re}\left(\lambda t_dD_2^*\right)^2+\mathrm{Im}\left(mt_sD_2^*\right)^2}\right]\\
&\quad-2i(1-x)\left[\mathrm{Im}\left(mt_sN_2^*\right)+4\,\mathrm{Im}\left(N_2D_2^*\right)+\frac{\mathrm{Im}\left(N_2D_2^*\right)^2\mathrm{Im}\left(mt_sD_2^*\right)}{\mathrm{Re}\left(\lambda t_dD_2^*\right)^2+\mathrm{Im}\left(mt_sD_2^*\right)^2}\right.\\
&\quad\left.-4\frac{\mathrm{Im}\left(N_2D_2^*\right)\mathrm{Re}\left(\lambda t_dD_2^*\right)^2}{\mathrm{Re}\left(\lambda t_dD_2^*\right)^2+\mathrm{Im}\left(mt_sD_2^*\right)^2}\right]\ ,
\end{aligned}\tag{A4}$$

resulting in the following expression for $T_1(1)$,

$$T_1(1)=\frac{4}{N_2N_2^*}\left(\mathrm{Re}\left(\lambda t_dN_2^*\right)-\frac{\mathrm{Im}\left(D_2^*N_2\right)^2\mathrm{Re}\left(\lambda t_dD_2^*\right)}{\mathrm{Re}\left(\lambda t_dD_2^*\right)^2+\mathrm{Im}\left(mt_sD_2^*\right)^2}\right)\ .\tag{A5}$$

Though we do not need it, we give an expression for the constant T_0, in terms of $T_2(x)$ an $T_1(x)$, for completeness

$$T_0=2\,\mathrm{Re}\left(T_2(0)/T_1(0)\right)T_1(1)-T_2(1)\ .\tag{A6}$$

ORCID iD

Eddy Ardonne https://orcid.org/0000-0003-4479-7106

References

[1] Agarwal K D, Konar T K, Lakkaraju L G C and Sen(De) A 2024 Detecting exceptional points through dynamics in non-Hermitian systems *Phys. Rev. A* **110** 012226
[2] Agarwal K D, Konar T K, Lakkaraju L G C and Sen(De) A 2023 Recognizing critical lines via entanglement in non-Hermitian systems (arXiv:2305.08374)
[3] Bergholtz E J, Budich J C and Kunst F K 2021 Exceptional topology of Non-Hermitian systems *Rev. Mod. Phys.* **93** 015005
[4] Braghini D, de Lima V D, Beli D, Rosa M I N and Arruda J R F 2022 Non-Hermitian acoustic waveguides with periodic electroacoustic feedback (arXiv:2210.05948)
[5] Brody D C 2014 Biorthogonal quantum mechanics *J. Phys. A: Math. Theor.* **47** 035305
[6] Delplace P, Yoshida T and Hatsugai Y 2021 Symmetry-protected multifold exceptional points and their topological characterization *Phys. Rev. Lett.* **127** 186602
[7] Edvardsson E 2022 Bulk-boundary correspondence and biorthogonality in nonHermitian systems *PhD Thesis* Stockholm University
[8] Edvardsson E, Kunst F K and Bergholtz E J 2019 Non-Hermitian extensions of higher-order topological phases and their biorthogonal bulk-boundary correspondence *Phys. Rev. B* **99** 081302(R)
[9] Ezawa M 2019 Braiding of Majorana-like corner states in electric circuits and its non-Hermitian generalization *Phys. Rev. B* **100** 045407
[10] Ezawa M 2024 Even-odd effect on robustness of Majorana edge states in short Kitaev chains *Phys. Rev. B* **109** L161404
[11] Gong Z, Ashida Y, Kawabata K, Takasan K, Higashikawa S and Ueda M 2018 Topological phases of non-Hermitian systems *Phys. Rev. X* **8** 031079
[12] Kawabata K, Bessho T and Sato M 2019 Classification of exceptional points and non-Hermitian topological semimetals *Phys. Rev. Lett.* **123** 066405
[13] Kawabata K, Shiozaki K, Ueda M and Sato M 2019 Symmetry and topology in non-Hermitian physics *Phys. Rev. X* **9** 041015
[14] Koch R and Budich J C 2020 Bulk-boundary correspondence in non-Hermitian systems: Stability analysis for generalized boundary conditions *Eur. Phys. J. D* **74** 70
[15] Kunst F K and Dwivedi V 2019 Non-Hermitian systems and topology: a transfer-matrix perspective *Phys. Rev. B* **99** 245116
[16] Kunst F K, Edvardsson E, Budich J C and Bergholtz E J 2018 Biorthogonal bulk-boundary correspondence in non-Hermitian systems *Phys. Rev. Lett.* **121** 026808
[17] Mandal I 2024 Non-Hermitian generalizations of the Yao-Lee model augmented by SO(3)-symmetry-breaking terms *APL Quantum* **1** 036104
[18] Mandal I 2024 Identifying gap-closings in open non-Hermitian systems by Biorthogonal polarization *J. Appl. Phys.* **135** 094402
[19] Mandal I and Bergholtz E J 2021 Symmetry and higher-order exceptional points *Phys. Rev. Lett.* **127** 186601
[20] Manna S and Roy B 2023 Inner skin effects on non-Hermitian topological fractals *Commun. Phys.* **6** 10
[21] Martinez Alvarez V M, Barrios Vargas J E and Foa Torres L E F 2018 Non-Hermitian robust edge states in one dimension: Anomalous localization and eigenspace condensation at exceptional points *Phys. Rev. B* **97** 121401(R)
[22] Larson J and Qvarfort S 2023 Exceptional points and exponential sensitivity for periodically driven Lindblad equations *Open Syst. Inf. Dyn.* **30** 2350008
[23] Lee T E 2016 Anomalous edge state in a non-Hermitian lattice *Phys. Rev. Lett.* **116** 133903
[24] Lee C H, Li L and Gong J 2019 Hybrid higher-order skin-topological modes in nonreciprocal systems *Phys. Rev. Lett.* **123** 016805
[25] Leykam D, Bliokh K Y, Huang C, Chong Y D and Nori F 2017 Edge modes, degeneracies and topological numbers in non-Hermitian systems *Phys. Rev. Lett.* **118** 040401
[26] Li J, Wang Y C, Duan L W and Chen Q H 2024 The PT-symmetric quantum Rabi model: Solutions and exceptional points (arXiv:2402.09749)

[27] Li L, Wei Y, Wu G, Ruan Y, Chen S, Lee C H and Ni Z 2024 Exact solutions disentangle higher-order topology in 2D non-Hermitian lattices (arXiv:2410.15763)
[28] Lin R and Li L 2024 Topologically compatible non-Hermitian skin effect *Phys. Rev. B* **109** 155137
[29] Lin R, Tai T, Yang M, Li L and Lee C H 2023 Topological Non-Hermitian skin effect *Front. Phys.* **18** 53605
[30] Liu C-C, Li L-H and An J 2023 Topological invariant for multi-band non-Hermitian systems with chiral symmetry *Phys. Rev. B* **107** 245107
[31] Maddi A, Auregan Y, Penelet G, Pagneux V and Achilleos V 2024 Exact analogue of the Hatano-Nelson model in 1D continuous nonreciprocal systems *Phys. Rev. Res.* **6** L012061
[32] Molignini P, Arandes O and Bergholtz E J 2023 Anomalous Skin Effects in Disordered Systems with a Single non-Hermitian Impurity *Phys. Rev. Res.* **5** 033058
[33] Nehra R and Roy D 2024 Anomalous dynamical response of non-Hermitian topological phases *Phys. Rev. B* **109** 094311
[34] Okuma N, Kawabata K, Shiozaki K and Sato M 2020 Topological origin of non-Hermitian skin effects *Phys. Rev. Lett.* **124** 086801
[35] Ortega-Taberner C and Hermanns M 2023 From Hermitian critical to non-Hermitian point-gapped phases *Phys. Rev. B* **107** 235112
[36] Nehra R and Roy D 2022 Topology of multipartite non-Hermitian one-dimensional systems *Phys. Rev. B* **105** 195407
[37] Rafi-Ul-Islam S M, Siu Z B, Razo M S H and Jalil M B A 2024 Dynamic manipulation of non-Hermitian skin effect through frequency in topolectrical circuits (arXiv:2410.16914)
[38] Rødland L, Ortega-Taberner C, Agarwal M and Hermanns M 2024 Disorder and non-Hermiticity in Kitaev spin liquids with a Majorana Fermi surface *Phys. Rev. B* **109** 155162
[39] Sarkar S, Ciccarello F, Carollo A and Bayat A 2024 Critical non-Hermitian topology induced quantum sensing *New J. Phys.* **26** 073010
[40] Shen H, Zhen B and Fu L 2018 Topological band theory for non-Hermitian Hamiltonians *Phys. Rev. Lett.* **120** 146402
[41] Stålhammar M and Bergholtz E J 2021 Classification of exceptional nodal topologies protected by PT symmetry *Phys. Rev. B* **104** L201104
[42] Vyas V M and Roy D 2021 Topological aspects of periodically driven non-Hermitian Su-Schrieffer-Heeger model *Phys. Rev. B* **103** 075441
[43] Yang F and Bergholtz E J 2024 Anatomy of higher-order non-Hermitian skin and boundary modes (arXiv:2405.03750)
[44] Yang K and Mandal I 2023 Enhanced eigenvector sensitivity and algebraic classification of sublattice-symmetric exceptional points *Phys. Rev. B* **107** 144304
[45] Yang F, Molignini P and Bergholtz E J 2023 Dissipative boundary state preparation *Phys. Rev. Res.* **5** 043229
[46] Yao S and Wang Z 2018 Edge states and topological invariants of non-Hermitian systems *Phys. Rev. Lett.* **121** 086803
[47] Yoshida T, Peters R, Kawakami N and Hatsugai Y 2019 Symmetry-protected exceptional rings in two-dimensional correlated systems with chiral symmetry *Phys. Rev. B* **99** 121101(R)
[48] Xiao L, Deng T, Wang K, Zhu G, Wang Z, Yi W and Xue P 2020 Non-Hermitian bulk-boundary correspondence in quantum dynamics *Nat. Phys.* **16** 761
[49] Xiong Y 2018 Why does bulk boundary correspondence fail in some non-Hermitian topological models *J. Phys. Commun.* **2** 035043
[50] Zelenayova M and Bergholtz E J 2024 Non-Hermitian extended midgap states and bound states in the continuum *Appl. Phys. Lett.* **124** 041105
[51] Zhang X, Song X, Zhang S, Zhang T, Liao Y, Cai X and Li J 2024 Solvable non-Hermitian skin effects and realspace exceptional points: non-Hermitian generalized Bloch theorem *J. Phys. A: Math. Theor.* **57** 125001
[52] Zhou H and Lee J Y 2019 Periodic table for topological bands with non-Hermitian symmetries *Phys. Rev. B* **99** 235112
[53] Herviou L, Bardarson J H and Regnault N 2019 Defining a bulk-edge correspondence for non-Hermitian Hamiltonians via singular-value decomposition *Phys. Rev. A* **99** 052118
[54] Longhi S 2019 Probing non-Hermitian skin effect and non-Bloch phase transitions *Phys. Rev. Res.* **1** 023013
[55] Lee C H and Thomale R 2019 Anatomy of skin modes and topology in non-Hermitian systems *Phys. Rev. B* **99** 201103

[56] Liu T, Zhang Y-R, Ai Q, Gong Z, Kawabata K, Ueda M and Nori F 2019 Second-order topological phases in non-Hermitian systems *Phys. Rev. Lett.* **122** 076801
[57] Fleckenstein C, Zorzato A, Varjas D, Bergholtz E J, Bardarson J H and Tiwari A 2022 Non-Hermitian topology in monitored quantum circuits (arXiv:2201.05341)
[58] Zirnstein H-G, Refael G and Rosenow B 2021 Bulk-boundary correspondence for non-Hermitian Hamiltonians via green functions *Phys. Rev. Lett.* **126** 216407
[59] Borgnia D S, Kruchkov A J and Slager R-J 2020 Non-Hermitian boundary modes and topology *Phys. Rev. Lett.* **124** 056802
[60] Yokomizo K and Murakami S 2019 Non-bloch band theory of non-Hermitian systems *Phys. Rev. Lett.* **123** 066404
[61] Yang K, Morampudi S C and Bergholtz E J 2021 Exceptional spin liquids from couplings to the environment *Phys. Rev. Lett.* **126** 077201
[62] Edvardsson E, Kunst F K, Yoshida T and Bergholtz E J 2020 Phase transitions and generalized biorthogonal polarization in non-Hermitian systems *Phys. Rev. Res.* **2** 043046
[63] Schomerus H 2020 Nonreciprocal response theory of non-Hermitian mechanical metamaterials: response phase transition from the skin effect of zero modes *Phys. Rev. Res.* **2** 013058
[64] Brzezicki W and Hyart T 2019 Hidden Chern number in one-dimensional non-Hermitian chiral-symmetric systems *Phys. Rev. B* **100** 161105(R)
[65] Edvardsson E and Ardonne E 2022 Sensitivity of non-Hermitian systems *Phys. Rev. B* **106** 115107
[66] Kitaev A Y 2001 Unpaired majorana fermions in quantum wires *Phys.-Usp.* **44** 131
[67] Alicea J 2012 New directions in the pursuit of Majorana fermions in solid state systems *Rep. Prog. Phys.* **75** 076501
[68] Yuce C 2016 Majorana edge modes with gain and loss *Phys. Rev. A* **93** 062130
[69] Klett M, Cartarius H, Dast D, Main J and Wunner G 2017 Relation between *PT*-symmetry breaking and topologically nontrivial phases in the Su-Schrieffer-Heeger and Kitaev models *Phys. Rev. A* **95** 053626
[70] Li C, Zhang X Z, Zhang G and Song Z 2018 Topological phases in a Kitaev chain with imbalanced pairing *Phys. Rev. B* **97** 115436
[71] Li C, Jin L and Song Z 2020 Coalescing Majorana edge modes in non-Hermitian *PT*-symmetric Kitaev chain *Sci. Rep.* **10** 6807
[72] Kawabata K, Ashida Y, Katsura H and Ueda M 2018 Parity-time-symmetric topological superconductor *Phys. Rev. B* **98** 085116
[73] Lieu S 2019 Non-Hermitian Majorana modes protect degenerate steady states *Phys. Rev. B* **100** 085110
[74] Yang X M and Song Z 2020 Resonant generation of a *p*-wave Cooper pair in a non-Hermitian Kitaev chain at the exceptional point *Phys. Rev. A* **102** 022219
[75] Zhao X-M, Guo C-X, Kou S-P, Zhuang L and Liu W-M 2021 Defective Majorana zero modes in non-Hermitian Kitaev chain *Phys. Rev. B* **104** 205131
[76] Sakaguchi T, Nishijima H and Takane Y 2022 Bulk-boundary correspondence and boundary zero modes in a non-Hermitian Kitaev Chain Model *J. Phys. Soc. Japan* **91** 124711
[77] Sayyad S and Lado J L 2023 Topological phase diagrams of exactly solvable non-Hermitian interacting Kitaev chains *Phys. Rev. Res.* **5** L022046
[78] Shi Y B and Song Z 2023 Fixed lines in a non-Hermitian Kitaev chain with spatially balanced pairing processes *Phys. Rev. B* **108** 125121
[79] Li B, Wang H-R, Song F and Wang Z 2024 Non-Bloch dynamics and topology in a classical nonequilibrium process *Phys. Rev. B* **109** L201121
[80] Rahul S, Roy N, Kumar R R, Kartik Y R and Sarkar S 2023 Unconventional quantum criticality in a non–Hermitian extended Kitaev chain *Sci. Rep.* **13** 12121
[81] Zhou L 2024 Entanglement Phase Transitions in Non-Hermitian Kitaev Chains *Entropy* **26** 272
[82] Mondal D and Nag T 2024 Persistent anomaly in dynamical quantum phase transition in long-range non-Hermitian p-wave Kitaev chain *Eur. Phys. J. B* **97** 59
[83] Fukui K, Kato Y and Motome Y 2024 Magnetic field effects on the Kitaev model coupled to environment *Phys. Rev. B* **110** 024429
[84] Pino D M, Meir Y and Aguado R 2024 Thermodynamics of Non-Hermitian Josephson junctions with exceptional points (arXiv:2405.02387)
[85] Cayao J and Aguado R 2024 Non-Hermitian minimal Kitaev chains (arXiv:2406.18974)

[86] Li S, Liu M, Zhang Y, Tian R, Arzamasovs M and Liu B 2024 Anomalous symmetry-protected blockade of the skin effect in one-dimensional non-Hermitian lattice systems *Phys. Rev. A* **110** 042208
[87] Lieb E, Schultz T and Mattis D 1961 Two soluble models of an antiferromagnetic chain *Ann. Phys.* **16** 407
[88] Mahyaeh I and Ardonne E 2018 Ardonne Zero modes of the Kitaev chain with phase-gradients and longer range couplings *J. Phys. Commun.* **2** 045010
[89] Chebyshev P L 1853 *ThéOrie des méCanismes Connus Sous le nom de ParalléLogrammes (Imprimerie de l'Académie impéRiale des Sciences)*
[90] Hatano N and Nelson D R 1996 Localization transitions in non-Hermitian quantum mechanics *Phys. Rev. Lett.* **77** 570
[91] Hatano N and Nelson D R 1997 Vortex pinning and non-Hermitian quantum mechanics *Phys. Rev. B* **56** 8651
[92] Hatano N and Nelson D R 1998 Non-Hermitian delocalization and eigenfunctions *Phys. Rev. B* **58** 8384
[93] Viéte F 1970 *Opera Mathematica* (Franciscus van Schooten with commentaries) Reprint by Georg Olms Verlag, Hildesheim, New York
[94] Routh E J 1877 *A Treatise on the Stability of a Given State of Motion, Particularly Steady Motion* (Macmillan and co)
[95] Hurwitz A 1895 Ueber die Bedingungen, unter welchen eine Gleichung nur Wurzeln mit negativen reellen Theilen besitzt *Math. Ann.* **46** 273
[96] Sturm P C 1829 Mémoire sur la résolution des équations numériques *Bull. Sci. Férussac.* **11** 419 Collected Works of Charles François Sturm, Birkhäuser Basel (2009)
[97] Bistritz Y 2002 Zero location of polynomials with respect to the unit-circle unhampered by nonessential singularities *IEEE Trans. Circuits Syst. I* **49** 305
[98] Cohn A 1922 Über die Anzahl der Wurzeln einer algebraischen Gleichung in einem Kreise *Math. Z.* **14** 110